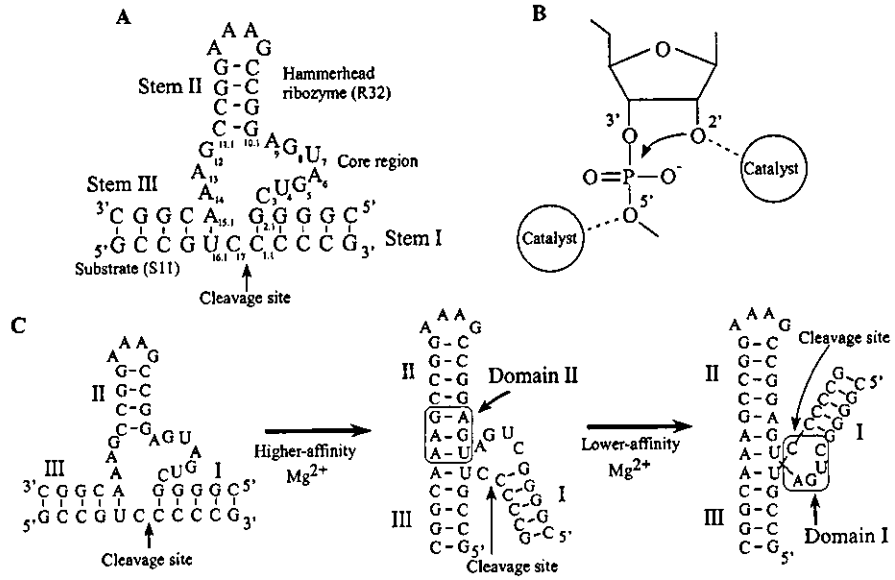


*Figure 1.* (A) Sequence and secondary structure of the hammerhead ribozyme (R32) and the substrate (S11) used in this study. (B) Schematic representation of the proposed mechanism of the hammerhead ribozyme reaction. The 2′-hydroxyl moiety is activated by the catalyst and then launches a nucleophilic attack on the adjacent phosphate, with subsequent cleavage of the bond at the 5′-oxygen. The developing negative charge on the leaving 5′-oxygen is stabilized by another catalyst. (C) Proposed two-stage scheme for folding of the ribozyme−substrate complex. The higher-affinity $Mg^{2+}$ ion(s) drives the formation of domain II, which includes non-Watson−Crick base pairs, and the lower-affinity $Mg^{2+}$ ion(s) rotates around helix I, forming the catalytic core.

ribozymes, which have generally been characterized as typical metalloenzymes, can no longer be categorized unambiguously.[26,36−38]

Hammerhead ribozymes, which act *in cis* during viral replication by the rolling circle mechanism, were identified originally in certain RNA viruses.[39] In the laboratory, ribozymes have been engineered such that they act on other RNA molecules *in trans* and catalyze the cleavage of phosphodiester bonds at specific sites to generate specific products, each of which has a 2′,3′-cyclic phosphate and a 5′-hydroxyl group (Figure 1A).[40−43] The transesterification reaction includes deprotonation of the 2′-hydroxyl moiety of a ribose group, nucleophilic attack of the 2′-oxygen on the adjacent phosphorus atom, and stabilization (neutralization) of the 5′-oxyanion leaving group (Figure 1B).[44] A large body of evidence also indicates that the P9/$G_{10.1}$ site binds a metal ion with high affinity, with other metal ion-binding sites being located around the $G_5$ nucleobase and the $A_{13}$ phosphate near the site of cleavage.[45−48] Thus, the idea that ribozymes are metalloenzymes has become generally accepted. However, it was reported recently that ribozymes are active in the presence of very high concentrations of monovalent cations, such as $Li^+$ or $NH_4^+$ ions, or at moderate (below 100 mM) concentrations of the exchange-inert complex ion $Co(NH_3)_6^{3+}$, in the absence of divalent metal ions.[26,37] These findings raise the possibility that it might be inappropriate to classify hammerhead ribozymes as metalloenzymes. By contrast, we observed a difference in numbers of protons transferred in the transition state between ribozyme-catalyzed reactions that were allowed to proceed in the presence of $Mg^{2+}$, $Li^+$, and $NH_4^+$ ions, and we proposed that the catalyst in the reaction might depend on the conditions of the reaction.[36,49−51]

Our previous kinetic analysis supported the "two-phase folding model" that was originally proposed by Lilley and coworkers (Figure 1C).[50,52−56] In this study, we examined the validity of the two-phase folding model and the reaction pathway by performing stoichiometric analyses of our hammerhead ribozyme's activity as a function of the concentration of different monovalent ions in the presence and in the absence of $Mg^{2+}$ ions. Our results strongly support the existence of the novel cooperative pathway in the hammerhead ribozyme reaction. We also found that our hammerhead ribozyme has a very unique characteristic with respect to the dependence of its reaction on $Mg^{2+}$ ions, even in the presence of approximately 1 M $Mg^{2+}$ ions. Such dependence suggests that the ribozyme's activity

(37) Curtis, E. A.; Bartel, D. P. *RNA* **2001**, *7*, 546−552.
(38) O'Rear, J. L.; Wang, S.; Feig, A. L.; Beigelman, L.; Uhlenbeck, O. C.; Herschlag, D. *RNA* **2001**, *7*, 537−545.
(39) Symons, R. H. *Annu. Rev. Biochem.* **1992**, *61*, 641−671.
(40) Uhlenbeck, O. C. *Nature* **1987**, *328*, 596−600.
(41) Haseloff, J.; Gerlach, W. L. *Nature* **1988**, *334*, 585−591.
(42) Hutchins, C. J.; Rathjen, P. D.; Forster, A. C.; Symons, R. H. *Nucleic Acids Res.* **1986**, *14*, 3627−3640.
(43) Koizumi, M.; Hayase, Y.; Iwai, S.; Kamiya, H.; Inoue, H.; Ohtsuka, E. *Nucleic Acids Res.* **1989**, *17*, 7059−7071.
(44) Zhou, D.-M.; Taira, K. *Chem. Rev.* **1998**, *98*, 991−1026.
(45) Wang, S.; Karbstein, K.; Peracchi, A.; Beigelman, L.; Herschlag, D. *Biochemistry* **1999**, *38*, 14363−14378.
(46) Maderia, M.; Hunsicker, L. M.; DeRose, V. J. *Biochemistry* **2000**, *39*, 12113−12120.
(47) (a) Zhou D.-M.; Kumar, P. K. R.; Zhang, L.-H.; Taira, K. *J. Am. Chem. Soc.* **1996**, *118*, 8969−8970. (b) Yoshinari, K.; Taira, K. *Nucleic Acids Res.* **2000**, *28*, 1730−1742. (c) Suzumura, K.; Yoshinari, K.; Tanaka, Y.; Takagi, Y.; Kasai, Y.; Warashina, M.; Kuwabara, T.; Orita, M.; Taira, K. *J. Am. Chem. Soc.* **2002**, *124*, 8230−8236. (d) Warashina, M.; Kuwabara, T.; Nakamatsu, Y.; Takagi, Y.; Kato, Y.; Taira, K. *J. Am. Chem. Soc.* **2004**, *126*, XXXX−XXXX.
(48) Peracchi, A.; Beigelman, L.; Scott, E. C.; Uhlenbeck, O. C.; Herschlag, D. *J. Biol. Chem.* **1997**, *272*, 26822−26826.
(49) Sawata, S.; Komiyama, M.; Taira, K. *J. Am. Chem. Soc.* **1995**, *117*, 2357−2358.
(50) (a) Zhou, J.-M.; Zhou, D.-M.; Takagi, Y.; Kasai, Y.; Inoue, A.; Baba, T.; Taira, K. *Nucleic Acids Res.* **2002**, *30*, 2374−2382. (b) Inoue, A.; Takagi, Y.; Taira, K. *Nucleic Acids Res.* **2004**, *32*, 4217−4223. (c) Takagi, Y.; Ikeda, Y.; Taira, K. *Topics Curr. Chem.* **2004**, *232*, 213−251.
(51) Takagi, Y.; Taira, K. *J. Am. Chem. Soc.* **2002**, *124*, 3850−3852.
(52) Bassi, G. S.; Murchie, A. I. H.; Walter, F.; Clegg, R. M.; Lilley, D. M. J. *EMBO J.* **1997**, *16*, 7481−7489.
(53) Horton, T. E.; Clardy, D. R.; DeRose, V. J. *Biochemistry* **1998**, *37*, 18094−18101.
(54) Bassi, G. S.; Møllegaard, N. E.; Murchie, A. I. H.; Lilley, D. M. J. *Biochemistry* **1999**, *38*, 3345−3354.
(55) Hammann, C.; Norman, D. G.; Lilley, D. M. J. *Proc. Natl. Acad. Sci. U.S.A.* **2001**, *98*, 5503−5508.
(56) Bassi, G. S.; Møllegaard, N. E.; Murchie, A. I. H.; von Kitzing, E.; Lilley, D. M. J. *Nat. Struct. Biol.* **1995**, *2*, 45−55.

reaches more than 100 $min^{-1}$ at pH 8 and 25 °C in the presence of more than 800 mM $Mg^{2+}$ ions. Our ribozyme might, thus, be very suitable for studies of the mechanism of catalysis as is the very fast so-called "kissing ribozyme" reaction described by Khvorova et al.[57]

## Experimental Section

**Preparation of the Hammerhead Ribozyme and Substrate.** The ribozyme (R32) and its substrate (S11) were synthesized chemically on a DNA/RNA synthesizer (model 394; PE Applied Biosystems, Foster City, CA) using phosphoramidic chemistry with 2′-*tert*-butyldimethylsilyl (TBDMS) protection, as described elsewhere.[47] The chemically synthesized oligonucleotides R32 and S11 were deprotected by incubation in a mixture of 28% ammonia and ethanol (3:1, v/v) at 55 °C for 8 h. Each mixture was evaporated to dryness, and the residue was allowed to dissolve in 1 mL of 1 M tetrabutylammonium fluoride (TBAF; Sigma-Aldrich Japan K. K., Tokyo, Japan) at room temperature for 12 h. After the addition of 1 mL of water, the mixture was desalted on a gel-filtration column (Bio-Gel P-4; Bio-Rad Laboratories, Hercules, CA). Fully deprotected oligonucleotides were purified by gel electrophoresis on a 20% polyacrylamide gel that contained 7 M urea, the respective bands were excised from the gel, and oligonucleotides were extracted in water. The oligonucleotides were recovered by ethanol precipitation, and then solutions were desalted on a gel-filtration column (TSK-GEL G3000PW; TOSOH, Tokyo, Japan) with ultrapure water. The RNA oligomers were quantitated in terms of absorbance at 260 nm.

We radiolabeled the substrate S11 using [$\gamma$-$^{32}$P]-ATP and T4 polynucleotide kinase (TaKaRa Bio Inc., Shiga, Japan) and purified the radiolabeled S11 on a 20% polyacrylamide gel that contained 7 M urea. After purification by the standard procedure as described above, the preparation of S11 was desalted on a gel-filtration column (NAP-10 column; Amersham Biosciences K. K., Tokyo, Japan).

**Quantification of the Ribozyme Reaction.** All ribozyme reactions were performed under ribozyme-saturated single-turnover conditions to ensure that conversion of the ribozyme−substrate complex to the ribozyme−product complex could be monitored kinetically without complications due to complex formation and slow release of product in particular at a high concentration of metal ions. The solution for the ribozyme reaction contained a trace amount of 5′-$^{32}$P-labeled S11 in 25 mM Bis-Tris buffer at pH 6.0 or pH 7.5 and 25 °C. The pH values of all 1.25× stock Bis-Tris buffers that contained appropriate metal ions (metal-ion buffers) were adjusted appropriately with HCl, and we confirmed that each buffer had the appropriate pH under the chosen reaction conditions. The error in the reading of pH meter under very high concentrations of metal ions is expected to be negligible.[58] Each reaction was initiated by addition of the substrate to a mixture of metal-ion buffer and ribozyme, and aliquots were removed from the reaction mixture at appropriate intervals. Each aliquot was mixed with more than three volumes of a stop solution that contained 100 mM MES (pH 6), 100 mM EDTA, 7 M urea, xylene cyanol (0.1%), and bromophenol blue (0.1%), and then it was stored at −80 °C prior to analysis. Since EDTA is known not to chelate $Mg^{2+}$ ions efficiently at lower pH values and does not effectively chelate monovalent cations, we confirmed that reactions did not continue in the stop solution and that effective quenching was achieved as a result of the high concentration of urea in this solution. Uncleaved substrate and 5′-cleaved products were separated on a 20% polyacrylamide gel that contained 7 M urea. The extent of each cleavage reaction was quantitated with an image analyzer (Storm 830; Molecular Dynamics, Sunnyvale, CA). For each reaction, an observed rate constant was

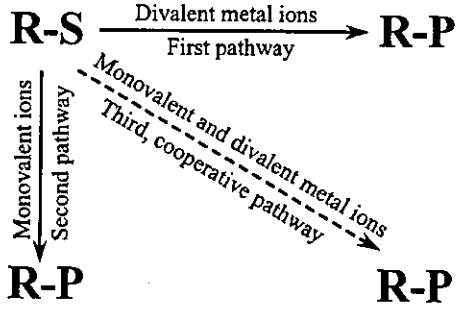


***Figure 2.*** Possible pathways in the hammerhead ribozyme reaction. R−S and R−P stand for the ribozyme−substrate complex and the ribozyme−product complex, respectively. The first pathway requires only divalent metal ions, such as $Mg^{2+}$ ions; the second pathway requires monovalent ions, such as $Li^+$ ions; and the third pathway involves both divalent and monovalent cations.

determined by nonlinear least-squares fitting of the time course of the reaction, using the following pseudo-first-order equation:

$$P_t = P_e - (P_e - P_0)\exp(-k_{obs}t)$$

where $P_t$ is the amount of a product at reaction time $t$ (min), $P_e$ is the amount of a product at the endpoint, $P_0$ is the amount of a product at the start of the reaction, and $k_{obs}$ is the observed rate constant ($min^{-1}$).

**The Basic Strategy for the Establishment of the Pathways of Reactions Catalyzed by the Hammerhead Ribozyme.** The basic strategy for establishment of the pathways of the reaction is shown in Figure 2. We suggested previously that a third pathway might be operative in the ribozyme reaction in addition to the two that have already been well characterized.[50] The first and second pathways involve only $Mg^{2+}$ ions and only $Li^+$ ions, respectively. The third pathway involves the cooperative effects of two kinds of metal ion. We first investigated the dependence of the reaction on either $Mg^{2+}$ or $Li^+$ ions independently and fitted the results to each scheme that has been postulated on the basis of our earlier data to choose values for basic parameters by nonlinear least-squares method. Finally, we established the third pathway on the basis of the reaction that occurred in the presence of the two metal ions, proceeding step by step and satisfying the parameters established in our analyses of the first and second pathways.

## Results and Discussion

**$Li^+$ Ions Have an Inhibitory Effect but Are Also a Better Accelerator Than Other Monovalent Ions of the Ribozyme Reaction in the Presence of $Mg^{2+}$ Ions.** We examined the activity of the hammerhead ribozyme as a function of the concentration of various monovalent metal ions, namely, $Li^+$, $Na^+$, $K^+$, $Cs^+$, and $NH_4^+$ in the presence of 10 mM $Mg^{2+}$ ions. The reactions were performed at pH 6 and 25 °C, at concentrations on monovalent cations from 0 to 3 M. As shown in Figure 3, all monovalent ions, the Group I metal ions and $NH_4^+$ ions, had an inhibitory effect at a few hundred mM in the presence of 10 mM $Mg^{2+}$ ions. This inhibitory effect can be explained by the simple hypothesis that monovalent ions prevent necessary binding of $Mg^{2+}$ ions to the ribozyme−substrate complex, as validated by DeRose and colleagues by EPR.[53]

In the case of $Li^+$, $Na^+$, and $NH_4^+$ ions, the ribozyme activity was elevated at higher concentrations of each monovalent ion individually. This observation is consistent with our previous observations of reactions in the presence of either $Mn^{2+}$ plus $Na^+$ ions or $Mg^{2+}$ plus $Na^+$ ions.[50] The inhibitory effect of $Na^+$ ions has also been observed in kinetic studies by other

(57) Khvorova, A.; Lescoute, A.; Westhof, E.; Jayasena, S. D. *Nat. Struct. Biol.* **2003**, *10*, 708−712.
(58) Millazo, G. *Elektrochemie*; Springer-Verlag: Berlin, 1952; p 98.

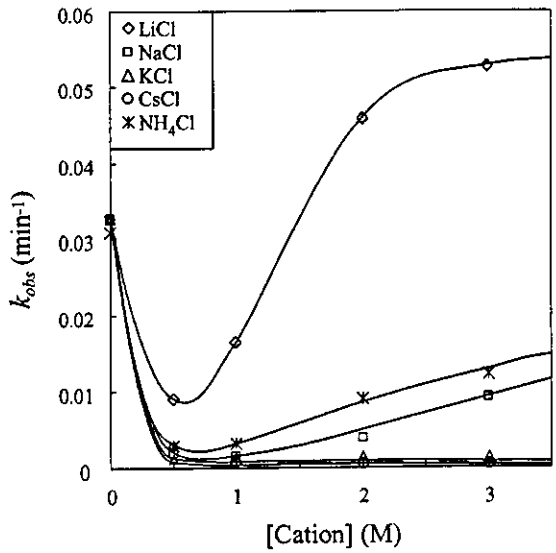


***Figure 3.*** Dependence on various monovalent ions of the activity of the hammerhead ribozyme (R32) in the presence of $Mg^{2+}$ ions. Values of $k_{obs}$ are plotted as a function of concentration of $Li^+$, $Na^+$, $K^+$, $Cs^+$, and $NH_4^+$ ions, respectively. All reactions were performed in the presence of 10 mM $Mg^{2+}$ ions under ribozyme-saturated single-turnover conditions at pH 6 and 25 °C. All monovalent ions had an inhibitory effect at 500 mM, and $Li^+$ ions accelerated the reaction at higher concentrations.

researchers at 100 mM $Na^+$ ions in the presence of $Mg^{2+}$ ions.[59] In addition to their inhibitory effect, $Li^+$ ions at higher concentrations were the best accelerator of the ribozyme reaction in the presence of $Mg^{2+}$ ions.

In the case of $K^+$ and $Cs^+$ ions, respectively, there was no acceleration of the reaction and both ions had the same effect (Figure 3). The rank order, in terms of the acceleration of ribozyme activity of the various monovalent ions in the presence of $Mg^{2+}$ ions, was rather similar to that of these monovalent ions in the absence of divalent metal ions (data not shown). As noted by Curtis and Bartel,[37] such dependence is correlated with the radius of each anhydrous ion and appears to be manifested even on a background of $Mg^{2+}$ ions (Figure 3).

It is particularly noteworthy that the observed accelerated activities were higher than the calculated sums of the activities in the presence of $Li^+$ ions and in the presence of $Mg^{2+}$ ions, suggesting that the divalent and monovalent ions act cooperatively in the reaction catalyzed by the hammerhead ribozyme (Figure 3).[50] We chose the combination of $Mg^{2+}$ and $Li^+$ ions for further stoichiometric analysis since it yielded the most pronounced profile in terms of inhibition and acceleration and the highest activities of all the combinations that we tested (Figure 3).

**The $Mg^{2+}$-Mediated Ribozyme Reaction and Elucidation of the First Pathway.** We examined the dependence on $Mg^{2+}$ ions of the activity of the hammerhead ribozyme up to a concentration of $Mg^{2+}$ ions close to 1 M at pH 6 and 25 °C under single-turnover conditions (ribozyme-saturating with respect to the substrate) to ensure that the kinetics of the cleavage reaction could be monitored without complications due to formation of the ribozyme–substrate complex and the slow release of products. As reported previously, the reaction in the presence of $Mg^{2+}$ ions is accelerated by increases in pH with a slope of unity.[36,44,60–62] Thus, we adjusted the pH of the reactions in this study to 6.0 to slow the reaction. Under these conditions, we were able to measure the rate constant of the rapid reaction precisely.

As shown in Figure 4A, we found an approximately first-order dependence on the concentration of $Mg^{2+}$ ions, and the rate constant did not reach a plateau value under our conditions, even at more than 800 mM $Mg^{2+}$ ions. The continuous increase in the rate constant with the addition of more and more $Mg^{2+}$ ions indicates the involvement of a $Mg^{2+}$ ion that has very low affinity for the hammerhead ribozyme–substrate complex. At 800 mM $Mg^{2+}$ ions, the rate constant approached 1 min$^{-1}$ at pH 6 and 25 °C, which is the limit of detection of a rapid cleavage reaction under standard laboratory conditions. The dependence of the activities of the hammerhead ribozymes on $Mg^{2+}$ ions has been studied by many researchers, generally of concentrations of $Mg^{2+}$ ions below 200 mM.[59–61,63,64] In most cases, the rate constant reached or approached a plateau value.[59,60,63] In this respect, our ribozyme exhibits unusual dependence on $Mg^{2+}$ ions.

Earlier analyses of the structure of hammerhead ribozymes and of the conformational changes caused by interactions with $Mg^{2+}$ ions suggested that major conformational changes occur in two stages, with the formation of domain II and then domain I, as indicated in Figure 1C.[52,54–56] The formation of domain II occurs first and results in the coaxial stacking of helices II and III. This conformational change is induced by the binding of a higher-affinity $Mg^{2+}$ ion(s) to the ribozyme–substrate complex. A divalent metal ion bound to the A9/$G_{10.1}$ site is a strong candidate for the ion that is involved in this first transition.[47d,65,66]

The second conformational change is the formation of the catalytic domain of the ribozyme, with movement of stem I toward stem II, and this change is induced by the binding of a lower-affinity $Mg^{2+}$ ion(s). The $K_d$ (equilibrium dissociation constant) of each transition has been investigated by various methods and appears to be several hundred micromolar and several millimolar for the first and the second transition, respectively.[52–56] Therefore, we chose 100 $\mu$M and 1 mM as $K_{d1}$ and $K_{d2}$, the fixed dissociation constants of the first and the second $Mg^{2+}$ ion(s), respectively, for the fitting in the first pathway (Figures 1C, 2, and 4B). The ribozyme reaction in the presence of high concentrations of $Mg^{2+}$ ions did not reach saturation. Therefore, we included additional $Mg^{2+}$ ions (indicated as $x$ $Mg^{2+}$) in the pathway, as shown in Figure 4B, and we fitted the reaction profiles to the following equation:

$$k_{obs} = \frac{\dfrac{[Mg^{2+}]^{(2+x)}}{K_{d1}K_{d2}K_{d6}}}{1 + \dfrac{[Mg^{2+}]}{K_{d1}} + \dfrac{[Mg^{2+}]^2}{K_{d1}K_{d2}} + \dfrac{[Mg^{2+}]^{(2+x)}}{K_{d1}K_{d2}K_{d6}}} k_1$$

where $K_{d6}$ is the dissociation constant of the additional $Mg^{2+}$

(59) Rueda, D.; Wick, K.; McDowell, S. E.; Walter, N. G. *Biochemistry* **2003**, *42*, 9924–9936.
(60) Dahm, S. C.; Derrick, W. B.; Uhlenbeck, O. C. *Biochemistry* **1993**, *32*, 13040–13045.
(61) Hendry, P.; McCall, M. J. *Nucleic Acids Res.* **1995**, *23*, 3928–3936.
(62) Peracchi, A. *Nucleic Acids Res.* **1999**, *27*, 2875–2882.
(63) (a) Kuimelis, R. G.; McLaughlin, L. W. *Biochemistry* **1996**, *35*, 5308–5317. (b) Hunsicker, L. M.; DeRose, V. J. *J. Inorg. Biochem.* **2000**, *80*, 271–281.
(64) Hampel, K. J.; Burke, J. M. *Biochemistry* **2003**, *42*, 4421–4429.
(65) DeRose V. J. *Curr. Opin. Struct. Biol.* **2003**, *13*, 317–324.

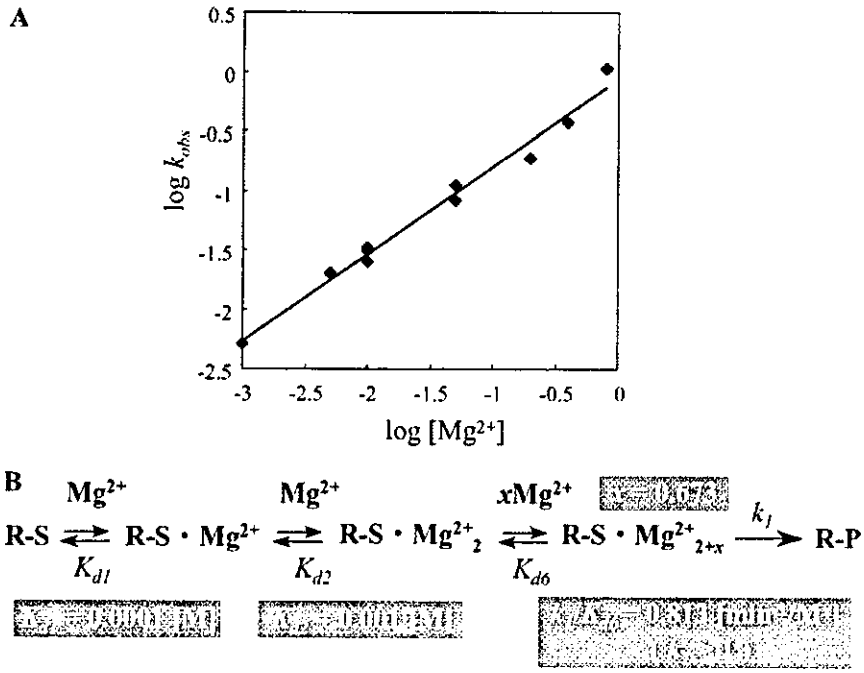


***Figure 4.*** (A) Dependence on $Mg^{2+}$ ions of the activity of the hammerhead ribozyme (R32). All reactions were performed at pH 6 and 25 °C under ribozyme-saturated single-turnover condition. The concentration of $Mg^{2+}$ ions ranged from 1 mM to 800 mM. The theoretical curve (– – –) as drawn after parameters had been fitted to the equation given in the text. (B) The first pathway, involving $Mg^{2+}$ ions, of the ribozyme reaction. R–S stands for the ribozyme–substrate complex. All parameters are explained in the text.

ion(s), $k_1$ is the rate constant for cleavage at a saturating concentration of $Mg^{2+}$ ions, and $x$ is the additional number of $Mg^{2+}$ ions.

Since the reaction did not reach saturation even at 800 mM $Mg^{2+}$ ions, we could not define $k_1$ and $K_{d6}$, but we were able to determine the values of $k_1/K_{d6}$ and $x$ after fitting the results to the equation. The calculated values of $k_1/K_{d6}$ and $x$ were 0.813 [$min^{-1}/M^x$] and 0.673, respectively. However, $k_1$ must be greater than 1 because $k_{obs}$ is close to 1 $min^{-1}$ at 800 mM $Mg^{2+}$ ($k_{obs}$ should be nearly equal to $k_1$ at saturating concentration of $Mg^{2+}$ ions). The theoretical curve, obtained after putting these results in the equation, is shown in Figure 4A.

At several hundred millimolar $Mg^{2+}$ ions, the formation of both domains II and I would be complete because of the low values of $K_{d1}$ and $K_{d2}$. If we take the global changes induced by the two types of $Mg^{2+}$ ion into consideration, it seems reasonable to conclude that the $Mg^{2+}$ ion with very low affinity that we detected might be involved in some step other than the formation of domains II and I. The step might be a further conformational change or the binding of a catalytic species to the ribozyme–substrate complex. Rueda et al. reported that a third and previously undetected metal ion at a rather high concentration might play a role in the induction of a minor conformational adjustment that leads to formation of the active state, after the formation of domains II and I.[59]

Although we are unable to calculate a Hill coefficient for $Mg^{2+}$ ions and cannot estimate the number of $Mg^{2+}$-binding sites from our current data, our results and those of others strongly support the possible existence of a very-low-affinity metal-binding site(s). Misra and Draper propose a model for the stabilization of RNA by $Mg^{2+}$ ions that involves two distinct binding modes, "diffuse binding" and "site binding".[67] Diffusely bound $Mg^{2+}$ ions are described as fully solvated $Mg^{2+}$ ions that interact with RNA through long-range electrostatic interactions exclusively. Site-bound $Mg^{2+}$ ions are described as partially desolvated ions that are attracted to electronegative pockets. In general, the affinity of diffusely bound $Mg^{2+}$ ions seems to be lower than that of site-bound $Mg^{2+}$ ions. Thus, it is possible that the very-low-affinity $Mg^{2+}$ ions that we detected might be involved in diffuse binding. Diffuse binding of metal ions appears, sometimes, to play a dominant role in the stabilization of the tertiary structures of small RNAs,[67] but it might also participate in the ribozyme reaction at some specific site(s) in the ribozyme–substrate complex.

The activity of the hammerhead ribozyme in 800 mM $Mg^{2+}$ ions is unusual because the observed rate constant is estimated to be about 100 $min^{-1}$ at pH 8 and 25 °C from the dependence on pH, which has a slope of unity as noted above. The rate constant at concentrations of $Mg^{2+}$ ions above 800 mM should be even higher because it is clear that 800 mM $Mg^{2+}$ is not a saturating concentration for the cleavage reaction. The rate constant approaches the estimated observed rate constant for the so-called "kissing ribozyme" at optimum conditions with respect to a concentration of $Mg^{2+}$ ions and pH.[57] The $Mg^{2+}$ ion has very low affinity for the ribozyme–substrate complex, and the number of truly active ribozyme species, at concentrations of $Mg^{2+}$ ions of several millimolar, is less than 1% of the number of ribozyme–substrate complexes (compare 1 $min^{-1}$ in 10 mM $MgCl_2$ at pH 8 and 25 °C[68] with 100 $min^{-1}$ in 800 mM $MgCl_2$ at the same pH and the same temperature).

**The $Li^+$-Mediated Ribozyme Reaction and Elucidation of the Second Pathway.** We examined the activity of the hammerhead ribozyme as a function of the concentration of $Li^+$

(66) Tanaka, Y.; Kasai, Y.; Mochizuki, S.; Wakisaka, A.; Morita, E. H.; Kojima, C.; Toyozawa, A.; Kondo, Y.; Taki, M.; Takagi, Y.; Inoue, A.; Yamasaki, K.; Taira, K. *J. Am. Chem. Soc.* **2004**, *126*, 744–752.

(67) Misra, V. K.; Draper, D. E. *J. Mol. Biol.* **2002**, *317*, 507–521.

(68) Stage-Zimmermann, T. K.; Uhlenbeck, O. C. *RNA* **1998**, *4*, 875–889.

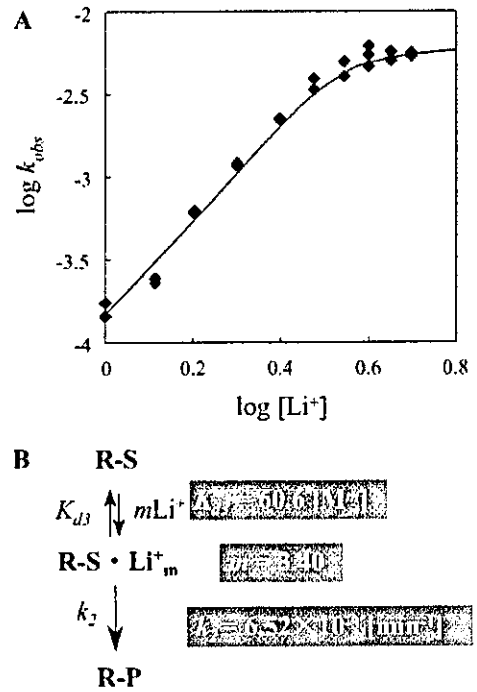


***Figure 5.*** (A) Dependence on $Li^+$ ions of the activity of the hammerhead ribozyme (R32) at pH 6. All reactions were performed at pH 7.5 and 25 °C under the ribozyme-saturated single-turn over conditions and the concentration of $Li^+$ ions ranged from 1 to 5 M. Data at pH 6 were extrapolated from the experimental data obtained at pH 7.5 as described in the text. The theoretical curve (−−) was drawn after parameters had been fitted to the equation given in the text. (B) The second pathway, involving $Li^+$ ions, of the hammerhead ribozyme reaction. R−S stands for the ribozyme−substrate complex. All parameters are explained in the text.

ions, in the absence of divalent metal ions, under ribozyme-saturating single-turnover conditions at pH 7.5 and 25 °C. The experimental data obtained at pH 7.5 were extrapolated to give results at pH 6 on the basis of the fact that the dependence of activity on pH has a slope of unity.[37,50b] The results are shown by diamonds in Figure 5A.

It is clear that the slope of the linear part of the curve in Figure 5A is steeper than that in Figure 4A (in the presence of $Mg^{2+}$ ions) and the activity reaches a plateau at high concentrations of $Li^+$ ions. Using the simple pathway shown in Figure 5B, we fitted the data to the following equation:

$$k_{obs} = \frac{\frac{[Li^+]^m}{K_{d3}}}{1 + \frac{[Li^+]^m}{K_{d3}}} k_2$$

where $m$ is the number of $Li^+$ ions, $K_{d3}$ is the dissociation constant of $Li^+$ ions, and $k_2$ is the rate constant for cleavage under $Li^+$-saturating conditions. The data fit well when $m$ = 3.40, $K_{d3}$ = 60.6 $M^m$, and $k_2 = 6.52 \times 10^{-3}$ $min^{-1}$ at pH 6. The theoretical curve obtained after fitting these values is shown in Figure 5A.

O'Rear et al. reported that the hammerhead reaction has second-order dependence on $Li^+$ ions, without a plateau.[38] By contrast, our ribozyme exhibited more than third-order dependence, and a plateau was observed (Figure 5A). Although there are some differences between our results and those of O'Rear et al., in both cases the order of dependence on $Li^+$ is greater than that on $Mg^{2+}$ ions, suggesting that $Li^+$ ions bind cooperatively to the ribozyme−substrate complex, while $Mg^{2+}$ ions bind sequentially.

From the value of $k_2$ at pH 7.5 and 25 °C, we recalculated the value at pH 6 and 25 °C (again, the ribozyme reaction is dependent, with a slope of a unity, on pH at high concentrations of $Li^+$ ions).[50b] We estimated $k_2$ to be $6.52 \times 10^{-3}$ $min^{-1}$ at pH 6 and 25 °C and used this value for stoichiometric analysis of the third pathway (see below).

**The Hammerhead Ribozyme Reaction in the Presence of $Mg^{2+}$ and $Li^+$ Ions and Characterization of the Third, Cooperative Pathway.** To characterize the third pathway, we examined the rate constant of the ribozyme reaction as a function of the concentration of $Mg^{2+}$ ions on a background of 2 M $Li^+$ ions and as a function of the concentration of $Li^+$ ions on a background of 10 mM $Mg^{2+}$ ions. All reactions were performed under ribozyme-saturating single-turnover conditions at pH 6 and 25 °C. The results are shown in Figure 6A,B. Parts A and B of the figure show apparent saturation at a high concentration of either $Mg^{2+}$ or $Li^+$ ions. We tested many possible third pathways for a good fit to these data, using the parameters of the first and second pathways that we had already fixed. We were able to identify a third, cooperative pathway that satisfied all the experimental data. The entire scheme, including the first, second, and third pathways, is shown in Figure 6C, and the corresponding equation is as follows:

$$k_{obs} = f_1 k_1 + f_2 k_2 + f_3 k_3$$

where

$$f_1 = \frac{1}{g} \cdot \frac{[Mg^{2+}]^{(2+x)}}{K_{d1} K_{d2} K_{d6}}$$

$$f_2 = \frac{1}{g} \cdot \frac{[Li^+]^m}{K_{d3}}$$

$$f_3 = \frac{1}{g} \cdot \frac{[Mg^{2+}]^{(1+y)}[Li^+]^{(n+n')}}{K_{d1} K_{d4} K_{d5} K_{d7}}$$

$$g = 1 + \frac{[Mg^{2+}]}{K_{d1}} + \frac{[Mg^{2+}]^2}{K_{d1}K_{d2}} + \frac{[Li^+]^m}{K_{d3}} + \frac{[Mg^{2+}][Li^+]^n}{K_{d1}K_{d4}} + \frac{[Mg^{2+}][Li^+]^{(n+n')}}{K_{d1}K_{d4}K_{d5}} + \frac{[Mg^{2+}]^{(2+x)}}{K_{d1}K_{d2}K_{d6}} + \frac{[Mg^{2+}]^{(1+y)}[Li^+]^{(n+n')}}{K_{d1}K_{d4}K_{d5}K_{d7}}$$

and where $n$ is the number of $Li^+$ ions as indicated in Figure 6C, $K_{d4}$ is the dissociation constant of these $n$ $Li^+$ ions, $n'$ is the number of further additional $Li^+$ ions as indicated in Figure 6C, $K_{d5}$ is the dissociation constant of these $n'$ $Li^+$ ions, $y$ is the number of $Mg^{2+}$ ions indicated in Figure 6C, $K_{d7}$ is the dissociation constant of these $y$ $Mg^{2+}$ ions, and $k_3$ is the rate constant for cleavage in the third pathway.

The third pathway involves interactions of $Mg^{2+}$ ions and $Li^+$ ions with the ribozyme−substrate complex. In the third pathway, $n$ $Li^+$ ions compete with a $Mg^{2+}$ ion (in the first pathway) to form a R−S·$Mg^{2+}$·$Li^+_n$ complex. This competition is the main cause of the observed inhibitory effect (Figure 3; see also below for details). Upon addition of more $Li^+$ ions, the relative activity of the first $Mg^{2+}$-only pathway becomes

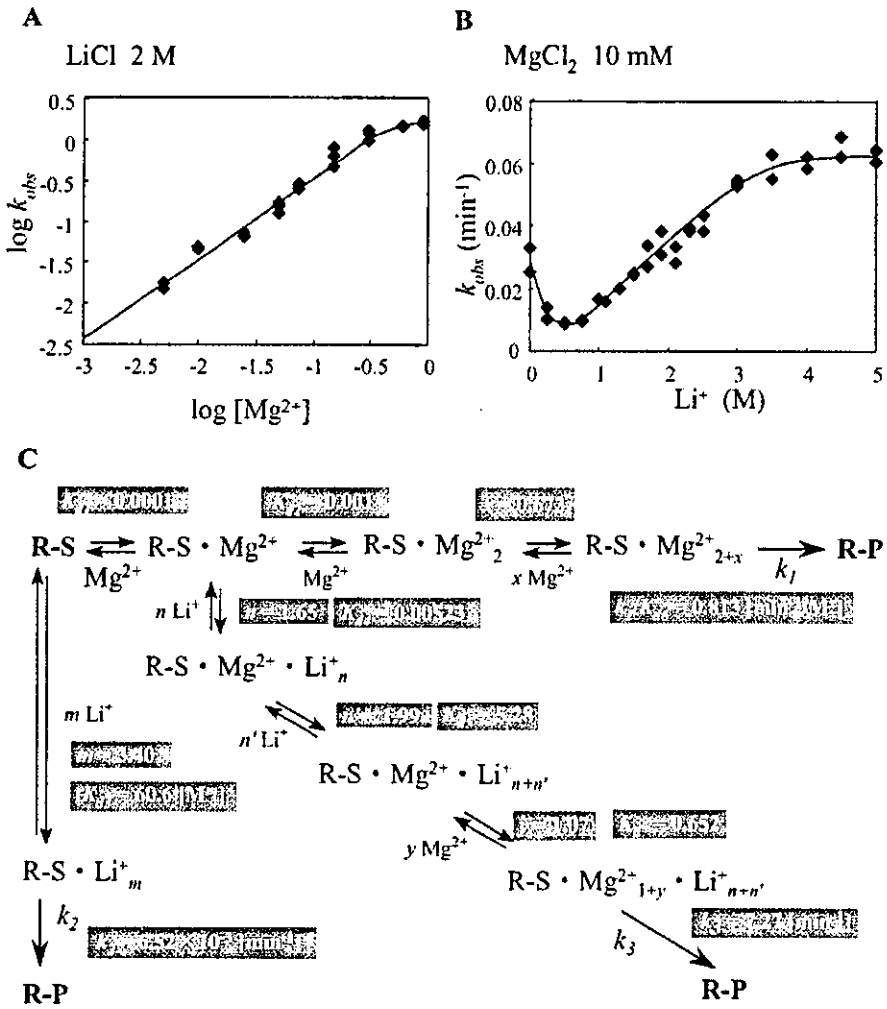


***Figure 6.*** (A) Dependence on $Mg^{2+}$ ions of the activity of the hammerhead ribozyme (R32) in the presence of 2 M $Li^+$ ions. All reactions were performed at pH 6 and 25 °C under the ribozyme-saturated single-turnover conditions and the concentration of $Mg^{2+}$ ions ranged from 5 mM to 800 mM. The theoretical curve (– – –) was drawn after parameters had been fitted to the equation given in the text. (B) Dependence on $Li^+$ ions of the activity of the hammerhead ribozyme (R32) on a background of 10 mM $Mg^{2+}$ ions. All reactions were performed at pH 6 and 25 °C under the ribozyme-saturated single-turnover conditions at concentration of $Li^+$ ions that ranged from 0 to 5 M. The theoretical curve (– – –) was drawn after parameters had been fitted to the equation given in the text. (C) The third pathway, involving both $Li^+$ and $Mg^{2+}$ ions, for the ribozyme reaction at pH 6 and 25 °C. R–S and R–P stand for complexes of the ribozyme–substrate and the ribozyme–product, respectively. All parameters are explained in the text.

smaller. We might imagine that the second $Li^+$-only pathway would become the major pathway upon addition of more $Li^+$ ions. However, the activity, indicated by $k_2$, of the second pathway is much lower than the $Mg^{2+}$-based rate, and the affinity of $Li^+$ ions for the ribozyme–substrate complex in the second pathway is very low.

Thus, the third cooperative pathway, instead of the second pathway, becomes the major pathway upon addition of more $Li^+$ ions. The R–S·$Mg^{2+}$·$Li^+_n$ complex is converted to a R–S·$Mg^{2+}$·$Li^+_{(n+n')}$ (Figure 6C) upon binding of $n'$ $Li^+$ ions. We then added $y$ $Mg^{2+}$ ions to the R–S·$Mg^{2+}$·$Li^+_{(n+n')}$ complex because we failed to obtain a good fit without the addition of such $Mg^{2+}$ ions. Thus, in the third pathway, two different metal ions, namely $(1+y)$ $Mg^{2+}$ ions and $(n+n')$ $Li^+$ ions, are involved in formation of the final complex. Using this model, we fit all the data to the equation and obtained by nonlinear least-squares method the following values: $n = 1.65$, $K_{d4} = 0.00523$, $n' = 1.99$, $K_{d5} = 5.28$, $y = 1.07$, $K_{d7} = 0.652$, and $k_3 = 7.27$ at pH 6 and 25 °C (Figure 6C).

The theoretical curves, obtained after inserting these parameters in the equation, are shown in Figure 6A,B. If we assume that $k_1$ is 1 $min^{-1}$ (this value is an underestimate because the reaction did not reach saturation even at 800 mM $Mg^{2+}$ ions; see above), the relative extent of each pathway on a background of $Mg^{2+}$ ions is as follows: 100% via the first pathway at 0 M $Li^+$ ions; 92% via the first pathway and 8% via the third pathway at 500 mM $Li^+$ ions; 48% via the first pathway and 52% via the third pathway at 1 M $Li^+$ ions; and 100% via the third pathway at 5 M $Li^+$ ions (Figure 7).

These parameters imply that (i) the pathway involving $Li^+$ ions alone (the second pathway) is negligible when both $Li^+$ and $Mg^{2+}$ ions are available (Figure 7A,B), (ii) an increase in the concentration of $Li^+$ ions on a background of $Mg^{2+}$ ions induces cooperation between $Li^+$ and $Mg^{2+}$ ions (the third pathway; Figure 7A), and (iii) an increase in the concentration of $Mg^{2+}$ ions on a background of $Li^+$ ions induces cooperation between $Li^+$ and $Mg^{2+}$ ions (the third pathway), although higher concentrations of $Mg^{2+}$ ions induce the first pathway and dramatically reduce the activity of the third pathway (Figure 7B). Simulations made on the assumption that $k_1$ is 5 or 10 $min^{-1}$ (rather than 1 $min^{-1}$) did not affect these conclusions. It should also be emphasized that, in the measurements of reaction

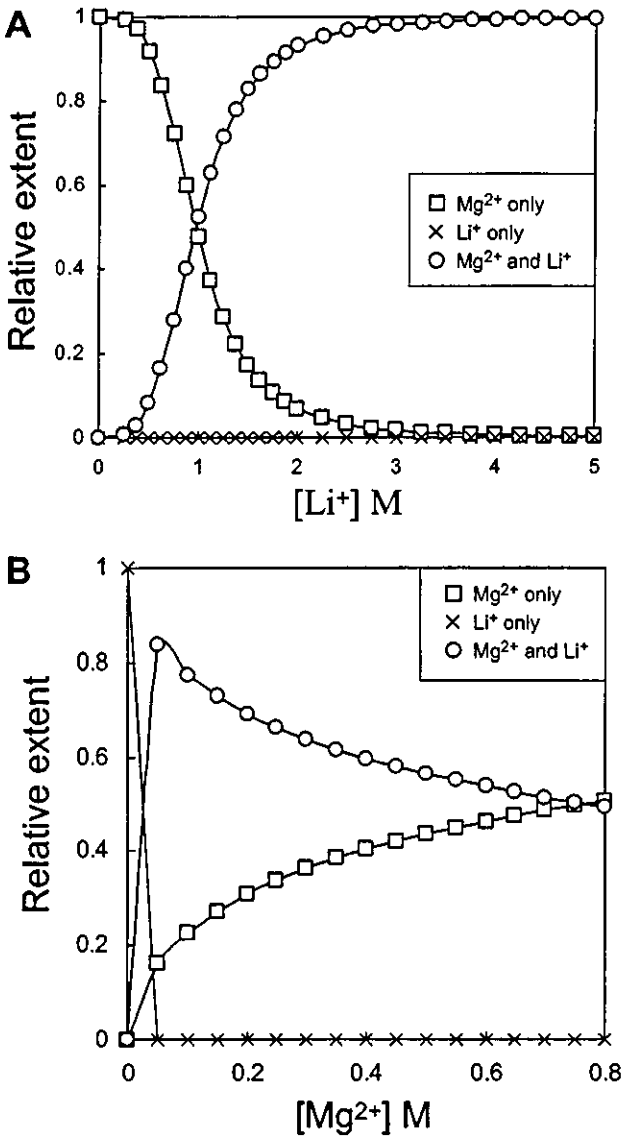


***Figure 7.*** Simulations showing the relative extent of involvement of each of the three pathways in the proposed scheme for hammerhead ribozyme reactions. The first pathway involved only $Mg^{2+}$ ions (□), the second pathway involved only $Li^+$ ions (×), and the third pathway involved both $Li^+$ and $Mg^{2+}$ ions (○). In this scheme, $k_1$ was taken as 1 $min^{-1}$. The relative values were obtained from calculations of $f_1$ ($Mg^{2+}$ alone), $f_2$ ($Li^+$ alone), and $f_3$ ($Mg^{2+}$ and $Li^+$; see the equations in the text) after fitting of the various parameters. (A) Simulation, in the presence of 10 mM $Mg^{2+}$ ions, of the relative extent of involvement of each pathway as a function of the concentration of $Li^+$ ions. (B) Similar simulations performed as a function of the concentration of $Mg^{2+}$ ions in the presence of 2 M $Li^+$ ions.

rates summarized in Figure 6C, we were unable to adjust the ionic strength at each concentration of metal ions because different cations we tested had differently affected the ribozyme reaction, as shown in Figure 3. Although we cannot exclude the possibility that the obtained parameters might have been influenced by the ionic strength, the major finding that the ribozyme reaction can proceed by a new cooperative pathway involving both monovalent and divalent metal ions remains valid.

**Comparison of Our Data with Previous Data.** In a previous report, we suggested the possible existence of various catalytic channels for the hammerhead ribozyme, depending on the reaction conditions. For example, a $Mg^{2+}$ ion functions as a catalyst in the transition state in $Mg^{2+}$-containing solutions while an $NH_4^+$ ion functions as a catalyst in $NH_4^+$-containing solutions.[51] Our data support an anhydrate direct interaction between these ions and the 5′-leaving oxygen atom at the cleavage site.[51]

However, since $Co(NH_3)_6^{3+}$ ions enhance the ribozyme's activity, we cannot exclude the possibility that, for example, a hydrated cation also functions as a catalyst in the transition state.[66] A multiple-channel model has also been proposed for reactions catalyzed by the HDV genomic ribozyme in which a base catalyst changes according to the environment in which the HDV ribozyme reaction occurs.[35] We propose similarly that several pathways are possible in the reaction catalyzed by hammerhead ribozymes. One of the pathways, the cooperative pathway, involves several different cations simultaneously. In the case of the reaction catalyzed by the RNA subunit of RNase P, similar cooperativity by $Mg^{2+}$ and $Ca^{2+}$ ions has been reported.[69]

Our data also suggest the existence of a very-low-affinity $Mg^{2+}$ ion (corresponding to $K_{d6}$ in Figures 4B and 6C), which was not included in the "two-phase folding model" proposed by Lilley and co-workers.[52,54-56] In a previous report, we postulated that this very-low-affinity $Mg^{2+}$ ion might play a catalytic or a structural role.[50] Rueda et al. reported recently that a third $Mg^{2+}$ ion might play a role, at a rather high concentration, in a minor conformational adjustment that results in formation of the active state after the formation of domains II and I (Figure 1C).[59] The $Mg^{2+}$ ion that we detected in the present study might be the same as the $Mg^{2+}$ ion that they discussed.

Our ribozyme did not yield a plateau even at 800 mM $Mg^{2+}$ ions (Figure 4A), while HHα (another hammerhead ribozyme that has been used in studies of reaction mechanisms by other researchers) yields a plateau at 100 mM $Mg^{2+}$ ions.[59] Breaker and co-workers proposed recently that a speed limit might exist for RNA-cleaving ribozymes that adopt $\alpha\gamma$ catalytic strategies, when the α, $\beta$, $\gamma$, and $\delta$ steps in catalysis are equivalent, respectively, to in-line nucleophilic attack, neutralization of negative charge on a nonbridging oxygen atom, deprotonation of the 2′-hydroxyl group, and neutralization of negative charge on the 5′-oxygen atom.[70,71] The reaction catalyzed by our hammerhead ribozyme cannot be categorized in terms of these steps because the $k_{max}$ of the reaction under optimal conditions can be extrapolated to exceed the speed limit of $\alpha\gamma$ catalysis at neutral pH and 25 °C (see above). This observation suggests the existence of some other catalytic strategy, for example, a $\delta$-metalation strategy or a $\beta$-metalation strategy. We noted earlier that no direct interaction occurs between a nonbridging oxygen atom and $Mg^{2+}$ ions at the cleavage site during cleavage by the hammerhead ribozyme,[47] while the direct coordination of a $Mg^{2+}$ ion to the 5′-leaving oxygen atom in the transition state was realized.[44,49,51] Thus, it appears that the hammerhead ribozyme exploits an $\alpha\gamma\delta_{metalation}$ strategy, rather than an $\alpha\beta_{metalation}\gamma$ strategy in $Mg^{2+}$-containing solutions. While this scenario might be valid in the $Mg^{2+}$-mediated ribozyme reaction, we cannot ignore the possibility that the same hammerhead

(69) Brännvall, M.; Kirsebom, L. A. *Proc. Natl. Acad. Sci. U.S.A.* **2001**, *98*, 12943−12947.
(70) Emilsson, G. M.; Nakamura, S.; Roth, A.; Breaker, R. R. *RNA* **2003**, *9*, 907−918.
(71) Breaker, R. R.; Emilsson, G. M.; Lazarev, D.; Nakamura, S.; Puskarz, I. J.; Roth, A.; Sudarsan, N. *RNA* **2003**, *9*, 949−957.

ribozyme might adopt a different strategy in a different environment.[51]

Rueda et al. reported that $Na^+$ ions had an inhibitory effect on the HHα ribozyme at 100 mM $Na^+$ ions on a background of $Mg^{2+}$ ions.[59] Hendry and McCall also reported the inhibitory effect on their hammerhead ribozyme of $Na^+$ ions on a background of $Mg^{2+}$ ions.[61] Such effects are consistent with our previous and current observations, namely, that inhibitory effects are greater at 500 mM $Na^+$ ions in the presence of a low concentration of $Mg^{2+}$ or $Mn^{2+}$ ions. However, the activity of our ribozyme can be restored by the addition of high concentrations of $K^+$ ions, $Na^+$ ions, or $Li^+$ ions (Figures 3 and 6B).[50] The activity of our ribozyme depended on the concentration of $Mg^{2+}$ ions even at around 1 M $Mg^{2+}$ ions. The observed rate constant of ~1 $min^{-1}$ at pH 6 and 25 °C in 800 mM $Mg^{2+}$ ions under single-turnover conditions allowed us to estimate that the ribozyme activity would be 100 $min^{-1}$ at pH 8. Since we observed no sign of saturation by $Mg^{2+}$ ions (Figure 4A), concentrations of $Mg^{2+}$ ions above 800 mM should lead to a rate constant greater than 100 $min^{-1}$ at pH 8. This rate constant is similar to that of the so-called "kissing ribozyme with the optimum activity" under optimum conditions with respect to a concentration of $Mg^{2+}$ ions and pH.[57]

## Conclusions

We have established a novel third pathway, namely, a cooperative pathway that involves monovalent and divalent metal ions, for the hammerhead ribozyme reaction. Moreover, complete kinetic parameters were obtained that explain the ribozyme activities under different conditions. The ribozyme reaction is more complex than might have been expected, perhaps because of the flexibility of RNA, which would have enhanced the potential of RNA during evolution of and in the RNA world. Our ribozyme, used as a model, might mimic the chemical cleavage of the so-called "kissing ribozyme with the optimum activity" because there was no upper limit to the rate constant of cleavage even at high concentrations of $Mg^{2+}$ ions. Further studies with our ribozyme might help to elucidate the catalytic mechanism of the "kissing ribozyme". Our analysis further indicates that the high concentrations of monovalent ions are inhibitory for the ribozyme in cells that is the disadvantage to the ribozyme compared to other catalysts such as siRNA whose activity can be enhanced by intracellular factors.

JA031991U

Published online August 27, 2004

4618–4629 Nucleic Acids Research, 2004, Vol. 32, No. 15
doi:10.1093/nar/gkh766

# Phosphorylation at 5′ end of guanosine stretches inhibits dimerization of G-quadruplexes and formation of a G-quadruplex interferes with the enzymatic activities of DNA enzymes

**M. Khabir Uddin[1], Yoshio Kato[1], Yasuomi Takagi[1,2], Toshiyasu Mikuma[1,4] and Kazunari Taira[1,2,3,*]**

[1]Gene Function Research Center and [2]iGENE Therapeutics, Inc., National Institute of Advanced Industrial Science and Technology (AIST), Central 4, 1-1-1 Higashi, Tsukuba Science City 305-8562, Japan, [3]Department of Chemistry and Biotechnology, School of Engineering, The University of Tokyo, Hongo, Tokyo 113-8656, Japan and [4]Department of Chemistry, University of Tsukuba, Tsukuba Science City 305-8571, Japan

Received February 2, 2004; Revised April 30, 2004; Accepted July 26, 2004

## ABSTRACT

**During an analysis of DNA enzymes by gel electrophoresis, we found that some DNA enzymes can adopt more than one conformation. The DNA enzyme Dz31 that formed more than one conformer contained a stretch of G residues. Further investigations, involving kinetic analysis and measurements of circular dichroism, indicated that this DNA enzyme and its derivatives formed G-quadruplexes. Moreover, we found that some derivative oligomers were capable of forming dimeric G-quadruplexes. We also compared the catalytic activities of Dz31 and its mutant derivatives. The present findings suggest that DNA enzymes with five or more continuous G residues are less favorable than those without $G_5$ in the association step in the enzymatic reaction and, thus, the choice of targets that contain a continuous stretch of C residues downstream of the cleavage site should be avoided. In addition, we found that negative charge–charge repulsion disrupted the dimerization of G-quadruplexes when a phosphate group was added directly to the 5′-terminal G of oligomers with continuous guanosine residues. In the case of 5′-phosphorylated $G_5$CTA, direct attachment of a phosphate group to the continuous $G_5$ sequence inhibited dimerization of G-quadruplexes, at least during electrophoresis on a denaturing gel.**

## INTRODUCTION

Unlike double-stranded DNA, single-stranded DNA can fold into well-defined, sequence-dependent tertiary structures; it can bind specifically to a variety of target molecules and it can exhibit catalytic activity similar to that of ribozymes or protein enzymes (1–3) even though no natural catalytic DNAs have been identified. DNA enzymes were discovered by *in vitro* selection procedures and were shown to catalyze chemical reactions, such as phosphoester transfer, phosphoester formation, porphyrin metalation, DNA capping and the cleavage of RNA or DNA, in the presence of divalent cations (4–10). Joyce's group and Breaker's group have developed DNA enzymes that can cleave RNAs in a sequence-specific manner and, thus, DNA enzymes may prove useful as inactivators of mRNAs of interest (11,12). The catalytic domain of a DNA enzyme is flanked by two substrate-recognition domains of seven or eight deoxyribonucleotides each, and the RNA substrate binds to the DNA enzyme through Watson–Crick base pairing (Figure 1). DNA enzymes can be complementary to ribozymes, such as hammerhead and hairpin ribozymes, and they have broad sequence-specificity and higher stability than RNA enzymes in cells. Therefore, it should be possible to utilize DNA to build new enzymes for applications both *in vitro* (13) and *in vivo* (14,15).

DNA enzymes have been engineered to act *in trans* against other RNA molecules and to catalyze the cleavage of phosphodiester bonds at specific sites to generate products with a 2′,3′-cyclic phosphate and a 5′-hydroxyl group (16). In previous studies, we showed that a DNA enzyme, designated as $DNAzyme_{(31mer)}$ or Dz3 (this DNA enzyme is referred to as Dz31 in the present paper; Figure 1) and directed against an $mRNA_{(17mer)}$ motif (b2a2), successfully cleaved its substrate at a specific position *in vivo* (14,15). The 17mer substrate designated b2a2 is a part of the *b2a2* mRNA that is transcribed from the Philadelphia chromosome, which results from reciprocal chromosomal translocations and produces cytogenetically abnormal cells in patients with chronic myelogenous leukemia (17). For our subsequent studies of structure–activity

*To whom correspondence should be addressed at Department of Chemistry and Biotechnology, School of Engineering, The University of Tokyo, Hongo, Tokyo 113-8656, Japan. Tel: +81 3 5841 8828 or +81 29 861 3015; Fax: +81 29 861 3019 or +81 3 5841 8828; Email: taira@chembio.t.u-tokyo.ac.jp
Correspondence may also be addressed to Yasuomi Takagi. Tel: +81 29 860 3203; Fax: +81 29 860 3205; Email: y-takagi@igene-therapeutics.co.jp

The authors wish it to be known that, in their opinion, the first three authors should be regarded as joint First Authors

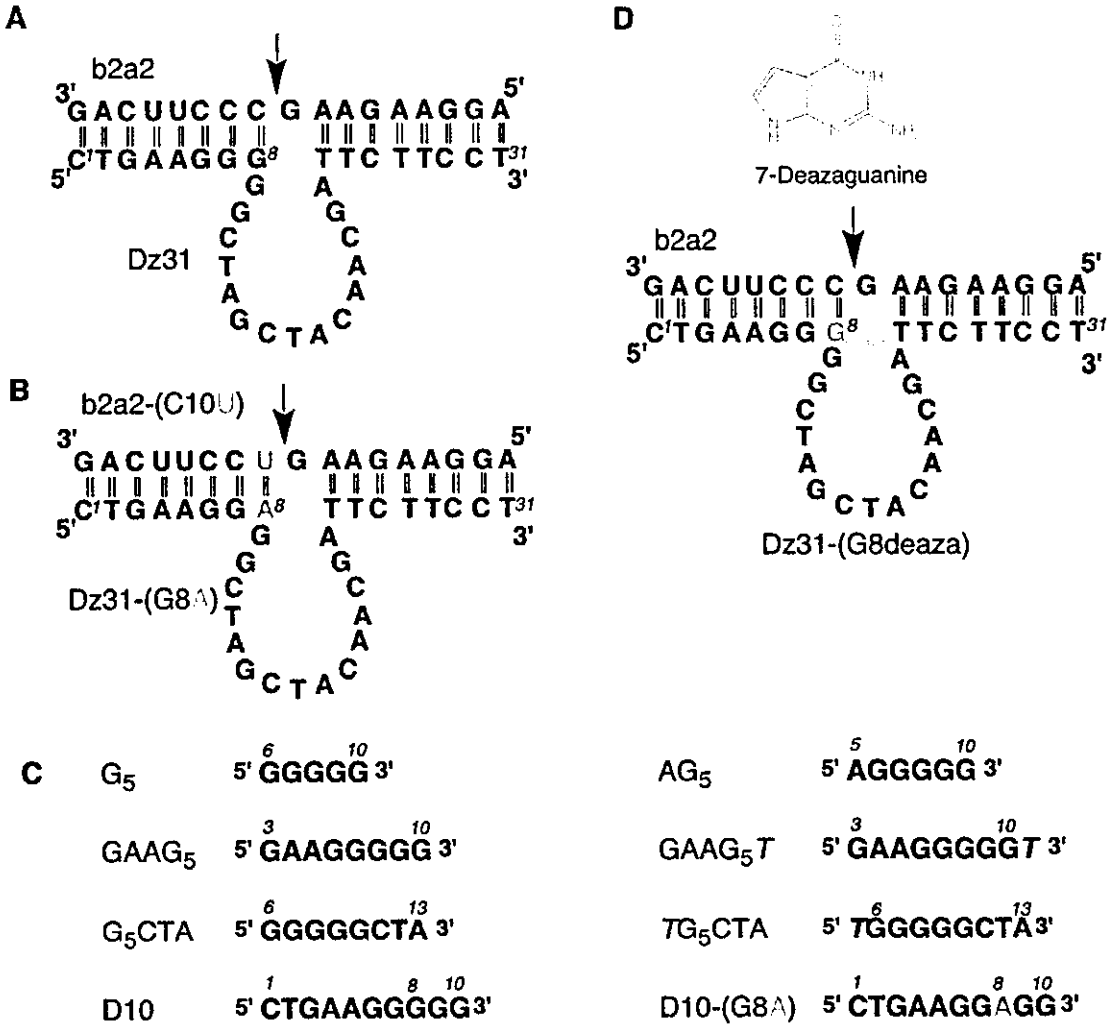


**Figure 1.** (A) Schematic representation of the DNA enzyme (Dz31) and its substrate (b2a2) [this enzyme was designated Dz3; (15)]. (B) The mutated DNA enzyme Dz31-(G8A) and its substrate b2a2-(C10U). (C) Segments of DNA enzymes that were examined by gel electrophoresis. (D) 7-Deazaguanine, the modified DNA enzyme Dz31-(G8deaza) and its substrate (b2a2), which were used in comparisons with wild-type Dz31.

relationships in the active core of DNA enzymes, we have focused on Dz31 and, during the present study, we found an unexpected complex, with lower mobility than expected, when we were checking the purity of Dz31 by gel electrophoresis.

In this study, we used gel electrophoresis and circular dichroism (CD) to identify the unexpected complex. We also investigated the activity of this complex in cleavage reactions. To compare the catalytic activities of Dz31, a mutated DNA enzyme$_{(31mer)}$ [Dz31-(G8A)] in which the central G within the continuous stretch of guanine nucleotides was replaced by A, and a modified DNA enzyme$_{(31mer)}$ [Dz31-(G8deaza)] in which hydrogen bonding within the stretch of G residues was disrupted, we designed substrates with an mRNA$_{(17mer)}$ motif (b2a2) and a modified mRNA$_{(17mer)}$ motif (b2a2-C10U) (Figure 1). We compared the activities of Dz31 and Dz31-(G8deaza) against the substrate with the mRNA$_{(17mer)}$ motif (b2a2) and examined the activity of Dz31-(G8A) against an mRNA$_{(17mer)}$ motif (b2a2-C10U). Dz31-(G8A), which differed from Dz31 only at the position of the eighth nucleotide (from the 5′ end) that is very important for the enzymatic reaction, was 50 times more active than Dz31 and Dz31-(G8deaza). The present findings suggest that DNA enzymes with a continuous stretch of five or more G residues participate inefficiently in the association step in the enzymatic reaction and that an adenosine at position 8 at the margin of the catalytic core of the DNA enzyme appears more suitable for effective activity than a guanine nucleotide at this position.

Guanine-rich sequences are found in biologically significant regions of the human genome, such as telomeres (18), immunoglobulin switch regions (19), gene promoter regions (20,21) and sequences associated with human diseases (22). A guanine quartet (G-quartet) is a cyclic array of four hydrogen-bonded guanine bases, in which each base is both the donor and acceptor of two hydrogen bonds with its neighbors through Hoogsteen-type base pairs. The core structure of the G-quadruplexes can be formed in many different ways, and many different structures have been observed. G-quadruplexes are known to be stable under certain conditions. In addition, G-quadruplexes are preferentially stabilized by metal ions. Monovalent ions typically interact predominantly with the negatively charged phosphate groups on DNA. However, in G-quartets, monovalent ions interact with eight carbonyl

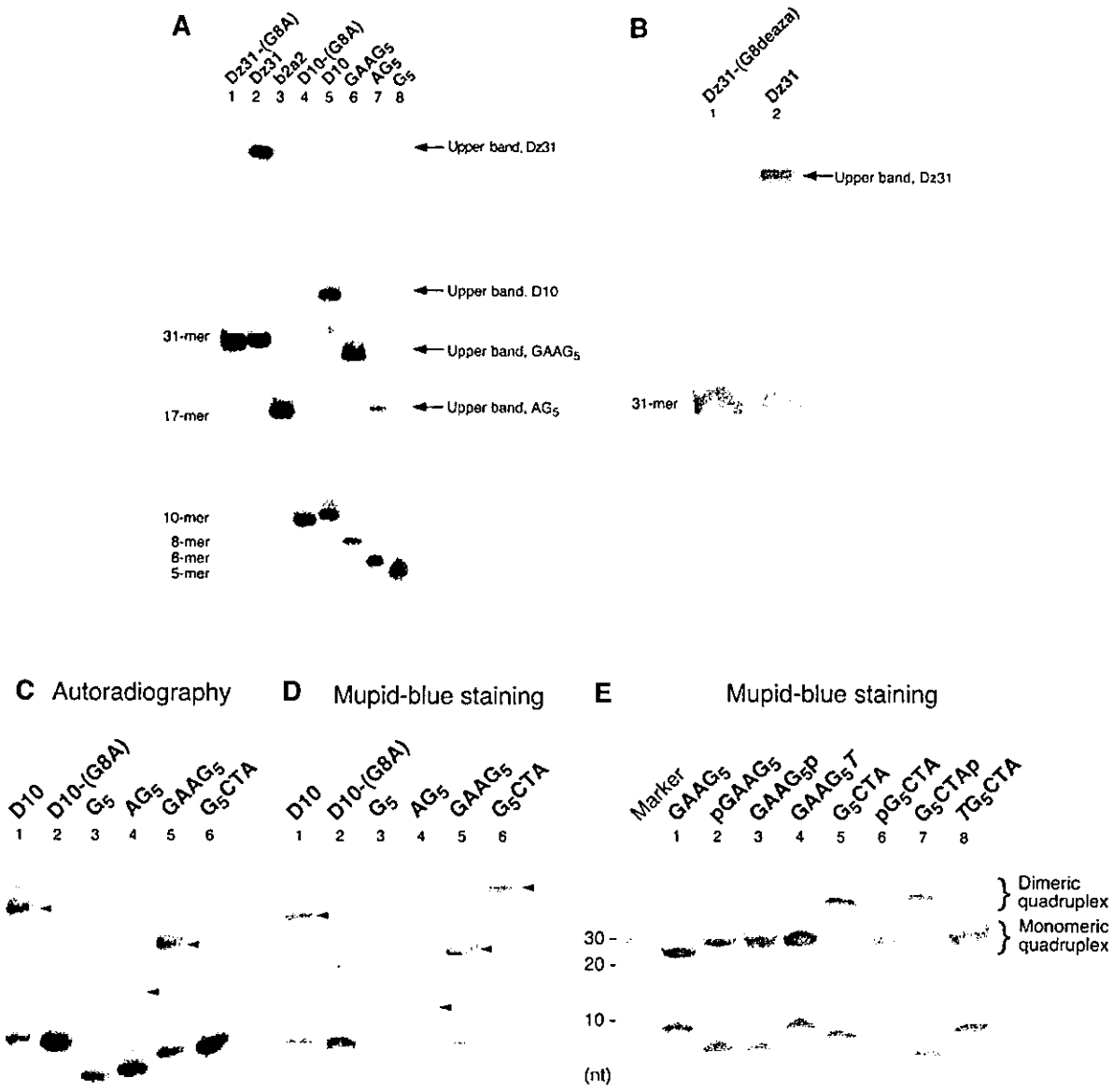


oxygen atoms. It is likely that the ion-binding properties of G-quadruplexes might be the most important contributor to their unique behavior (23).

The DNA enzyme$_{(31mer)}$ Dz31 and segments of this enzyme, namely, DNA$_{(10mer)}$ (D10), DNA$_{(8mer)}$ ($GAAG_5$) and DNA$_{(6mer)}$ ($AG_5$), which had a stretch of five continuous guanine nucleotides, each formed a band of lower mobility (upper band) during gel electrophoresis, as well as the expected band, whereas a modified DNA enzyme$_{(31mer)}$ [Dz31-(G8deaza)], a mutated DNA enzyme$_{(31mer)}$ [Dz31-(G8A)], and part of this enzyme DNA$_{(10mer)}$ [D10-(G8A)], which had no similar continuous stretch of guanine nucleotides, did not form an upper band. The measurements of CD revealed spectra typical of a G-quadruplex only in the case of oligomers with a continuous stretch of five guanine nucleotides. The CD data supported the results of gel electrophoresis and strongly suggested that the upper band on gels was due to the formation of a G-quadruplex. Importantly, some upper bands of derivative oligomers were found to be dimeric G-quadruplexes and their dimerization could be inhibited by 5′ phosphorylation.

## MATERIALS AND METHODS

### Synthesis and purification of substrates RNA$_{(17mer)}$ b2a2, RNA$_{(17mer)}$ b2a2-(C10U) and DNA oligomers

RNA oligonucleotides were synthesized on a DNA/RNA synthesizer (model 394; PE Applied Biosystems, Foster City, CA). The reagents for RNA synthesis were purchased from Glen Research (Sterling, VA). The crude deprotected oligonucleotides were purified on an open column and then purified on a 20% polyacrylamide gel that contained 7 M urea. Each band of interest was excised under ultraviolet irradiation, and RNA was eluted with milli-Q water (Millipore, Billerica, MA)

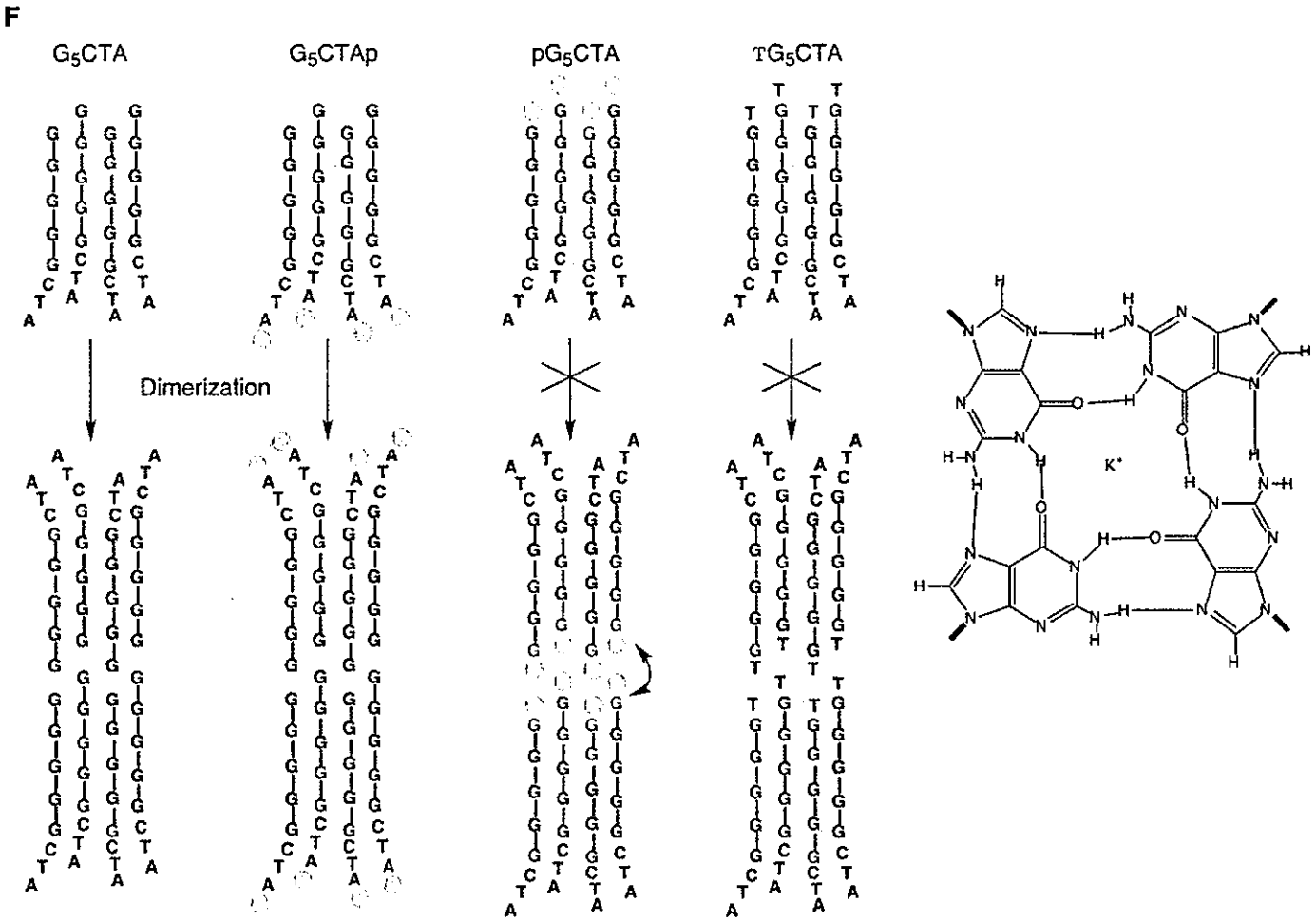


Figure 2. Gel electrophoretic analysis of the formation of G-quadruplexes. (A–C) 5′-$^{32}$P-labeled nucleotides were incubated at 4°C for 12 h in the presence of 100 mM KCl. Samples were subjected to electrophoresis on a denaturing 20% polyacrylamide gel in TBE buffer and detected by autoradiography. (D) The same gel used in (C) was stained with Mupid-Blue. Upper bands are indicated by arrowheads. (E) Non-labeled DNAs were subjected to electrophoresis and the gel was stained with Mupid-Blue. (F) Schematic representations of the effects of phosphorylation on the dimerization of a G-quadruplex. Phosphates at 5′-G terminus interfere the dimerization of G-quadruplexes.

followed by ethanol precipitation and desalted by passage through a NAP[10] column (Amersham Pharmacia Biotech AB, Uppsala, Sweden) that had been equilibrated with milli-Q water. Dz31-(G8deaza) was obtained from Japan Bio Service, Inc. (Saitama, Japan). Other DNAs were obtained from Hokkaido System Science Co., Ltd (Sapporo, Hokkaido, Japan) and Espec Oligo Service Corp. (Ibaraki, Japan). The DNAs were purified on a 20% polyacrylamide gel and preparations were desalted on a NAP[10] column.

### Gel electrophoresis

Gel electrophoresis was performed with $^{32}$P-labeled or non-labeled oligonucleotides. For the preparations of labeled samples, oligonucleotides were 5′ end-labeled with [γ-$^{32}$P]ATP using T4 polynucleotide kinase (Takara Bio, Inc., Shiga, Japan) and then mixed with unlabeled oligonucleotides to give appropriate final concentrations. Samples were analyzed on a 20% denaturing polyacrylamide gel that contained 100 mM KCl and have been equilibrated at 4°C for 3 h. Electrophoresis was performed in 100 mM Tris-borate buffer that contained 100 mM KCl overnight at room temperature. In the experiments with non-labeled oligomers, DNAs in 100 mM KCl were loaded onto 20% polyacrylamide gels without further processing, and then stained with Mupid-Blue (ADVANCE-BIO, Tokyo, Japan).

### CD measurements

Samples were dissolved in 10 mM sodium cacodylate, 100 mM KCl or 1 M urea, as necessary. The pH of each solution was adjusted to 6.7. CD spectra were recorded on a spectropolarimeter (J-820; Jasco, Tokyo, Japan) equipped with a temperature controller (PTC-423L; Jasco). For each sample, scans were performed over the range of wavelengths from 220 to 350 nm and a temperature range of 5–95°C in a cell with a 1 cm path length. The scan of each respective buffer was subtracted from the scan of each sample. The spectra were plotted in units of millidegrees versus wavelength and normalized to the total concentration of each species. The cell-holding chamber was flushed with a constant stream of dry nitrogen gas to avoid condensation of water on the exterior of the cell. All the

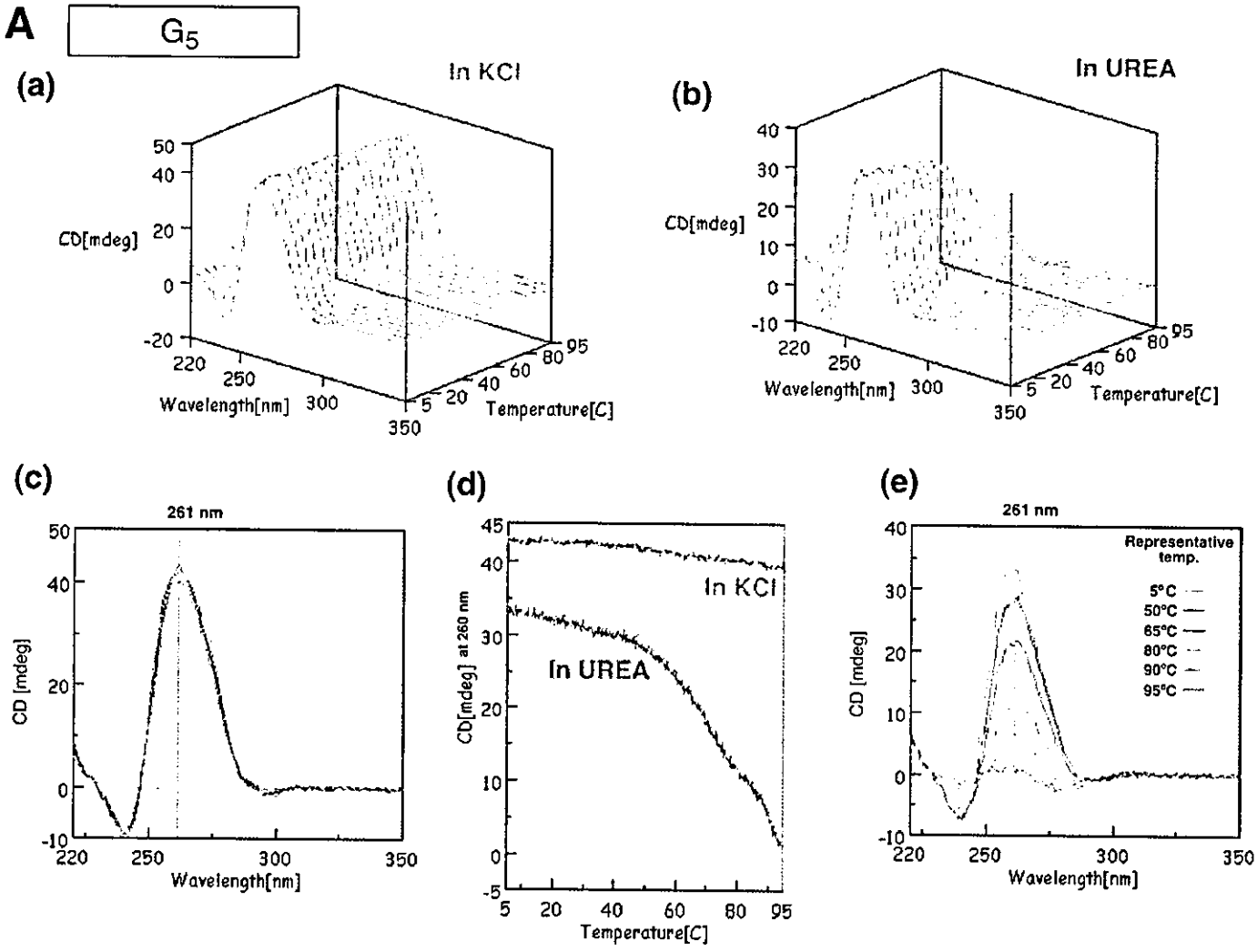


experiments were performed at least twice to confirm the reproducibility of results.

### Measurements of kinetic parameters

In general, reactions were initiated by the addition of metal ions and were stopped by the removal, at appropriate intervals, of aliquots of the reaction mixture, which were mixed with an equivalent volume of a solution that contained 100 mM EDTA, 9 M urea, 0.1% xylene cyanol and 0.1% bromophenol blue. The substrates were labeled with [$\gamma$-$^{32}$P]ATP by T4 polynucleotide kinase. Substrates and 5′-cleaved products were separated by electrophoresis on a 20% polyacrylamide/7 M urea denaturing gel and were detected by autoradiography. The extent of cleavage was determined by quantitation of radioactivity in the bands of substrate and product with a Bio-Image Analyzer (STORM; Molecular Dynamics, Sunnyvale, CA).

Assays of activities of Dz31 and Dz31-(G8deaza) were performed in 25 mM $MgCl_2$ and 50 mM Tris–HCl (pH 8.0) at 37°C, under single-turnover conditions, with incubations for 20, 40, 60, 120, 240 and 420 min. In the case of Dz31-(G8A), 50 mM Bis-Tris–HCl (pH 6.0) buffer was used and reaction mixtures were incubated for 5, 10, 20, 30, 60 and 120 min. To obtain kinetic parameters, we performed reactions under multiple-turnover conditions using 0.05–10 μM DNA enzyme, 1–200 μM RNA, 25 mM $MgCl_2$ and 50 mM Tris–HCl buffer (pH 8.0) at 37°C. Values of $K_m$ and $k_{cat}$ were calculated from Eadie–Hofstee plots.

## RESULTS AND DISCUSSION

### Formation and identification of a low-mobility form of DNA enzyme

We examined the formation of low-mobility forms (upper bands) of DNA enzymes and of segments of these enzymes by non-denaturing and denaturing PAGE (Figure 2). Figure 1 shows the sequences of DNA enzymes and the segments of these enzymes that we used in these experiments and their corresponding mobilities on a denaturing polyacrylamide gel are shown in Figure 2A and B. The mutant DNA enzyme Dz31-(G8A) (Figure 1B) and the modified DNA enzyme Dz31-(G8deaza) (Figure 1D) differed from the parental Dz31 (Figure 1A) in that the continuous stretch of five G residues was disrupted. In the experiments for which results are shown in Figure 2A and B, the oligonucleotides were denatured completely by heating at 96°C for 3 min, then they were allowed to equilibrate at the desired temperature

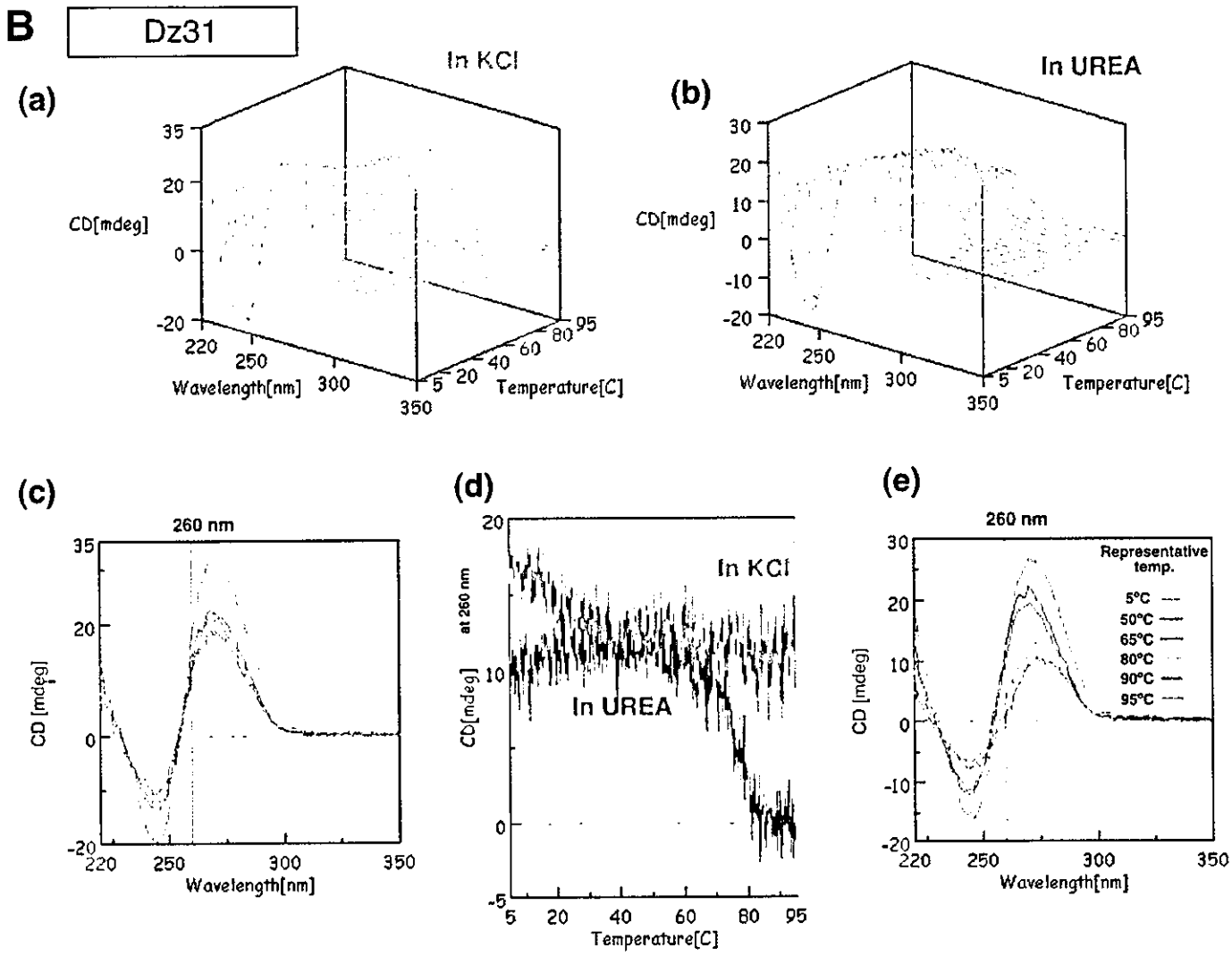


for 4 h in the presence of $K^+$ ions before being loaded onto 20% non-denaturing and denaturing polyacrylamide gels that were maintained at a specific temperature during electrophoresis. The samples were initially radiolabeled at their 5′ termini with [$\gamma$-$^{32}$P]ATP and purified by gel electrophoresis. Then, unlabeled oligonucleotides were mixed with labeled oligonucleotides to give the appropriate concentrations.

Dz31 and its derivatives, D10, $GAAG_5$ and $AG_5$, each yielded two bands during electrophoresis on a 20% non-denaturing gel in the absence of urea (data not shown). They also yielded two bands on a denaturing polyacrylamide gel in the presence of urea (Figure 2A). In contrast, Dz31-(G8A) and its derivative D10-(G8A) each yielded a single band (Figure 2A, lanes 1 and 4), as did Dz31-(G8deaza), on a denaturing gel (Figure 2B, lane 1). The mobilities of the lower bands indicated that the free oligonucleotides were of the expected size relative to that of the marker. The mobility of the upper band suggested that it was composed of material of 4 times the molecular weight of the material in the lower band. In other words, the mobility of a reference oligonucleotide with 4 times the molecular weight of Dz31 was almost the same as that of the material in the upper band (data not shown). According to the literature (23–25), our data suggested that the material in the upper band might have been a tetramer formed by intermolecular hydrogen bonding (Figure 2F).

To examine this hypothesis, we mutated to yield Dz31-(G8A) and its derivative D10-(G8A) at G8, the middle guanine nucleotide in the continuous stretch of five guanosine, changing G to A. In Dz31-(G8deaza) (Figure 1D), this G residue was modified by 7-deazaguanine, which breaks the hydrogen bond between the imidazole nitrogen ($N^7$) and the exocyclic-amine group of another guanine nucleotide. This mutation prevented the appearance of an upper band (Figure 2B). Therefore, it appeared that the upper bands were due to the five adjacent guanine nucleotides in the sequences, which should easily form a G-quadruplex as a result of intermolecular aggregation (23–28). Thawing and melting increased the intensity of the upper band of both Dz31 and its derivatives (data not shown), in agreement with previously reported results (29).

### Interference with dimerization of G-quadruplexes by terminal phosphate groups

To enhance our understanding of the formation of G-quadruplexes, we also examined several oligonucleotides

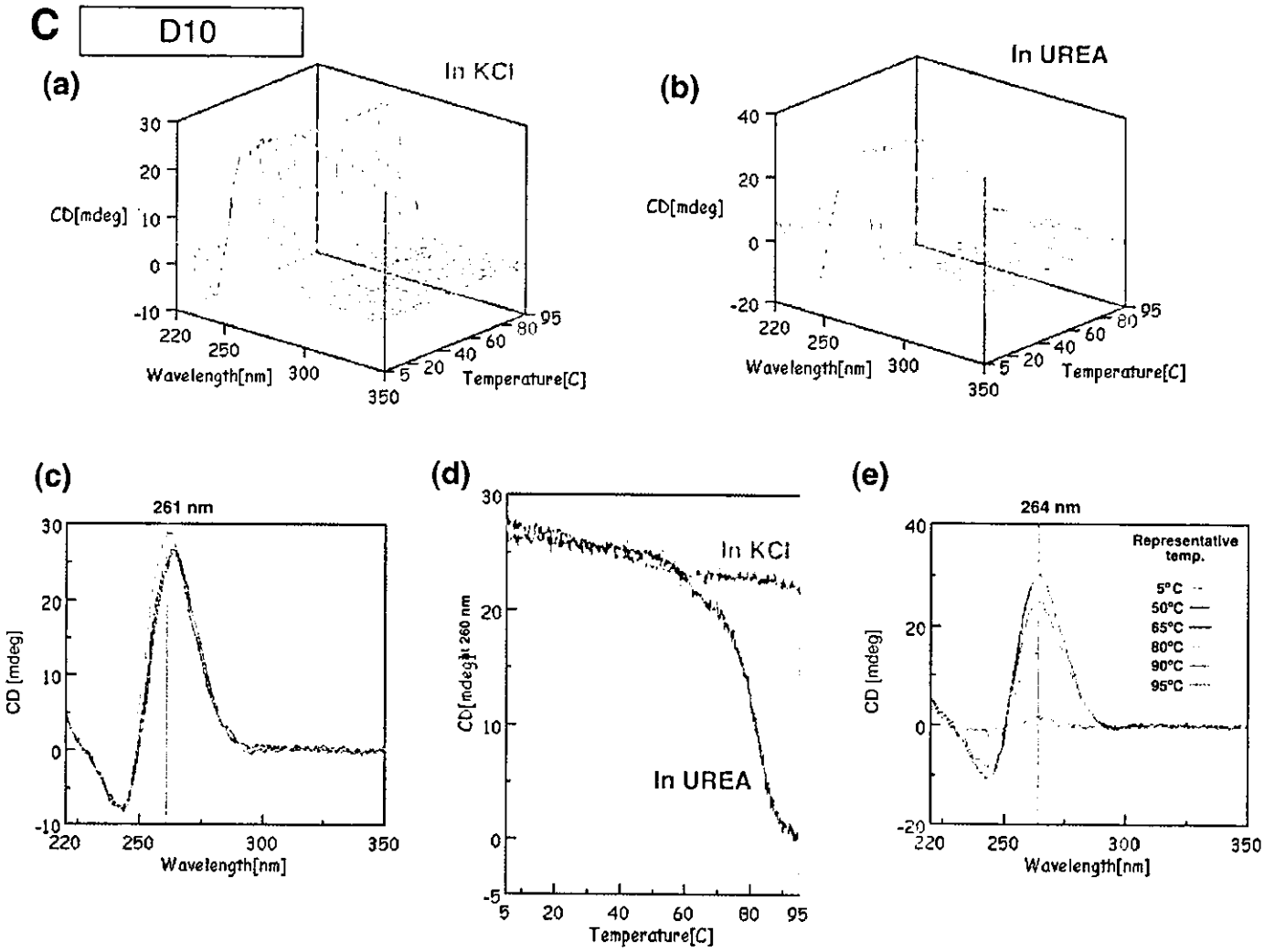


whose sequences were derived from Dz31. For the preparation of the phosphorylated oligomers shown in Figure 2C, we used T4 polynucleotide kinase to label oligomers with [$\gamma$-$^{32}$P]ATP. As shown in Figure 2C, $GAAG_5$ formed an upper band, but $G_5CTA$ and $G_5$ did not. It is probable that negative charge–charge repulsion disrupted the formation of a G-quadruplex when a phosphate group was added directly to the 5′-terminal G of a stretch of four or more guanosine residues. In fact, Figure 2C shows that no upper bands were formed by $G_5CTA$ and $G_5$, which might have a phosphate group at the 5′-terminal end of the $G_5$ region.

In the experiments for which results are shown in Figure 2D, we used the new reagent Mupid-Blue for the high-sensitivity detection of non-labeled oligomers. In contrast to the apparent absence of a G-quadruplex in Figure 2C, staining with Mupid-Blue indicated that $GAAG_5$ and $G_5CTA$ yielded upper bands in each case, probably a result of the formation of a parallel G-quadruplex (Figure 2D, lanes 5 and 6). Therefore, the absence of upper bands that corresponded to $G_5CTA$ and $G_5$ in Figure 2C was due to the fact that the T4 polynucleotide kinase was unable to attach phosphate groups to the termini of the G-quadruplexes and it was not due to disruption of the formation of a G-quadruplex by negative charge–charge repulsion.

To analyze the effect of phosphate groups, we prepared several oligomers with and without a phosphate group. The phosphorylated oligomers used in experiments for which results are shown in Figure 2E were synthesized by chemical addition of a phosphate group at the 5′ or 3′ end. As shown in Figure 2E, upper bands were detected in cases of $GAAG_5$ (lanes 1–3) and $G_5CTA$ (lanes 5–7) with or without a terminal phosphate.

Although the formation of these G-quadruplexes was very reasonable with 'G-continuous' DNAs, we did note an unexpectedly large difference in terms of electrophoretic mobility between $G_5CTA$ and $pG_5CTA$ (Figure 2E, lanes 5 and 6). We postulated that the G-quadruplexes formed by four molecules of $G_5CTA$ might form a dimeric G-quadruplex (two molecules of G-quadruplexes), as shown in Figure 2F. Since this kind of head-to-head dimerization of two sets of G-quadruplexes is known to be inhibited by the addition of one thymine nucleotide at the 5′ terminus (30–32) and in an attempt to explain the difference in mobilities, we prepared a one-thymine-nucleotide-supplemented oligomer ($TG_5CTA$)

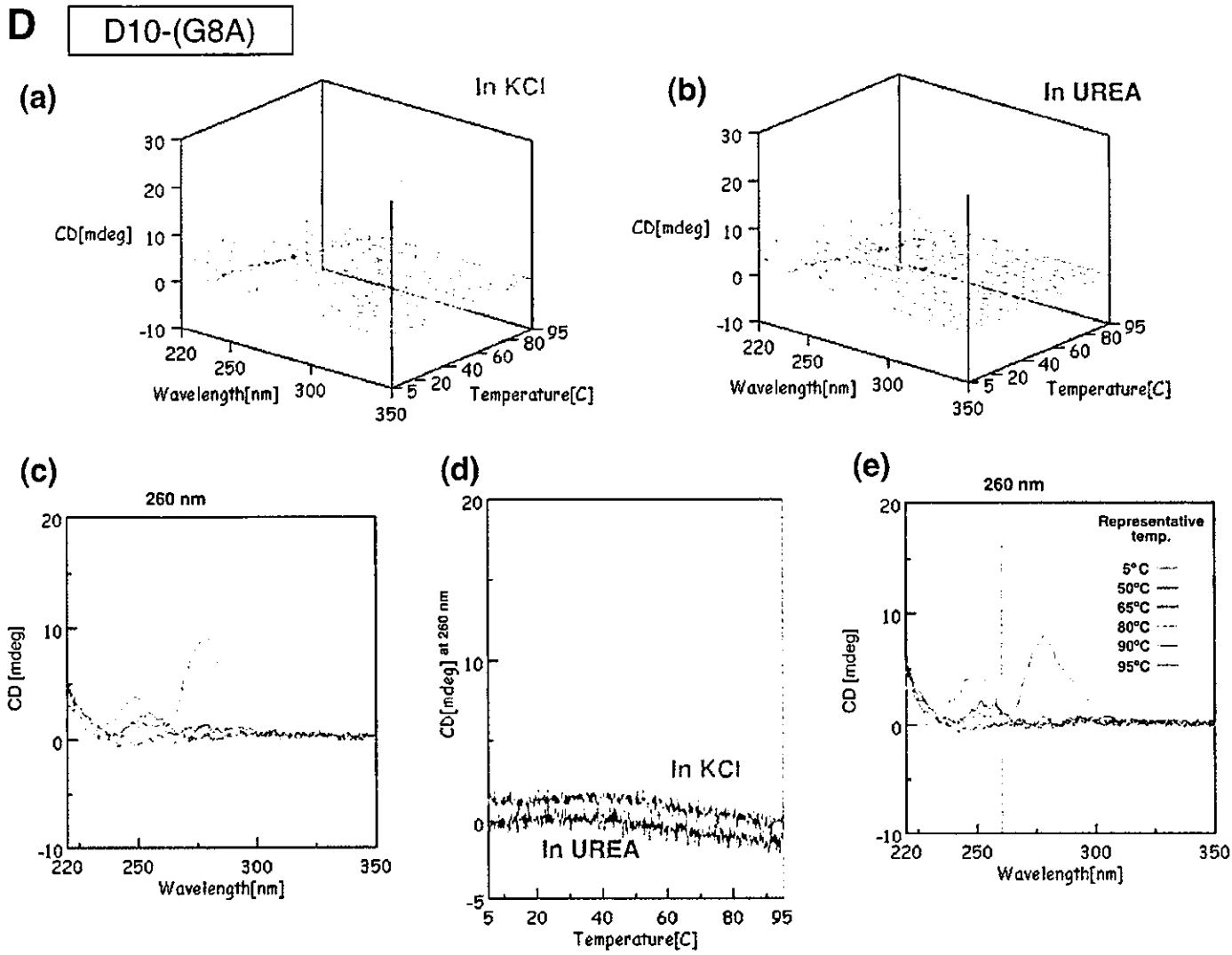


**Figure 3.** CD spectra of $G_5$ (**A**), Dz31 (**B**), D10 (**C**) and D10-(G8A) (**D**). Changes in spectra in KCl (a) and in urea (b) upon changes in temperature are shown. (c) The spectra in KCl are shown in two-dimensional graphs of CD (mdeg) versus wavelength (nm) at representative temperatures of 5, 50, 65, 80, 90 and 95°C. The vertical line exhibits the indicated wavelength, 260 or 261 nm. (d) Comparison of peak heights (mdeg) at 260 nm upon changes in temperature in KCl and in urea. (e) The spectra in urea as two-dimensional graphs of peak height (mdeg) versus wavelength (nm) at representative temperatures of 5, 50, 65, 80, 90 and 95°C. The vertical line exhibits the indicated wavelength, 260 or 261 nm.

and subjected it to gel electrophoretic analysis. We found that the mobility of $T$G$_5$CTA was almost identical to that of pG$_5$CTA, a monomeric G-quadruplex (Figure 2E). It appears that both $T$G$_5$CTA and pG$_5$CTA formed a simple parallel G-quadruplex.

While the reasons for these interesting phenomena are now somewhat clearer, several questions remain. The mobility of GAAG$_5$, which is potentially capable of forming a tail-to-tail dimeric G-quadruplex, was nearly the same as that of the monomeric G-quadruplex of GAAG$_5T$ (Figure 2E, lanes 1 and 4). It appears that GAAG$_5$ formed a simple parallel G-quadruplex in the same way as did GAAG$_5T$, despite the fact that most of the corresponding oligonucleotides examined in earlier similar studies formed a dimeric G-quadruplex with a 3′-G terminus (30–32). We are at present trying to examine this issue by analyzing many related derivatives.

Finally, although the newly discovered dimerization of the G-quadruplexes formed by G$_5$CTA is not unexpected, considering the G–G face interactions, it is noteworthy that the addition of a phosphate group at the 'G-terminal' end (pG$_5$CTA) interfered with the dimerization of G-quadruplexes, just as the addition of a thymidine disrupted the formation of dimers (Figure 2E and F). To our knowledge, this is the first demonstration of interference in the G–G face interactions by terminal phosphate groups.

### CD spectra of various oligomers

As noted above, the unexpected upper bands seen after gel electrophoresis seemed to be due to the formation of monomeric and dimeric G-quadruplexes. A simple way to confirm such a possibility is to record the CD spectra of such oligomers since a four-stranded quadruplex has a very specific spectrum that is due to the formation of a G-quadruplex. For example, parallel four-stranded quadruplexes are known to have a characteristic strong positive CD band at ~262 nm and a

negative band at 240 nm, whereas antiparallel folded quadruplexes have a positive band at 295 nm and a negative band at 260 nm (25). We applied this technique to the oligomers used in this study and confirmed that $G_5$ yielded spectral pattern of a parallel four-stranded quadruplex, as a positive control. As shown in Figure 3A(a), the spectra that we recorded coincided with those in previous reports by other groups, with a characteristic strong positive CD peak at 260–263 nm and a negative peak at 240 nm in the presence of 100 mM of KCl, at neutral pH, over a wide range of temperatures. In the presence of 1 M urea and ~10 mM NaCl (a component of the buffered solution) instead of 100 mM KCl, these strong peaks disappeared at higher temperatures, as shown in Figure 3A(b). This phenomenon was not unexpected since urea breaks hydrogen bonds between base pairs by interacting with functional groups of nucleobases. We defined the spectra and the changes in spectra with changes in temperature in the presence of 100 mM KCl or 1 M urea without $K^+$ ions as the criteria by which the presence or absence of a four-stranded quadruplex is assessed.

We monitored the CD spectra of Dz31 with changes in temperature in the presence of 100 mM KCl and in 1 M urea without $K^+$ ions. As shown in Figure 3B, strong positive and negative peaks were observed above 270 nm and above 240 nm, respectively, over the entire range of temperatures examined. These peaks did not disappear, even at 95°C and in the presence of 1 M urea. However, the value at 260 nm decreased dramatically, falling to zero in the case of urea, with a smaller decrease in the case of KCl, as shown in Figure 3B(c–e). Although the spectral patterns of Dz31 upon changes in temperature were somewhat ambiguous, the difference between the changes in intensities at 260 nm suggests the existence of a four-stranded quadruplex in the presence of KCl. The ambiguity might have been due to the existence of several other spectral forms, e.g. the catalytic core.

To facilitate our analysis, we decided to monitor the spectra of D10 at various temperatures. The sequence of the D10 motif is the same as that of the first 10 nt from the 5′ end of Dz31. The spectrum had strong positive and negative peaks at 261 and 240 nm respectively, as seen also in the spectrum of $G_5$ (Figure 3C). Thus, the region adjacent to the continuous stretch of five guanosine nucleotides in D10 did not affect the formation of parallel four-stranded quadruplexes in KCl. In the presence of 1 M urea without KCl, the heights of peaks at 264 and 240 nm fell to zero at higher temperatures, as seen also in the case of $G_5$ itself [Figure 3C(c–e)].

## Comparison of the results of CD spectroscopy and gel electrophoresis

As noted in our discussion of the results of gel electrophoresis, several oligomers containing five adjacent guanosine nucleotides, such as Dz31, D10, $GAAG_5$ and $AG_5$, yielded unexpected bands with reduced mobility, as well as the expected bands, during electrophoresis, namely, 'upper bands' (Figure 2A). These oligomers yielded similar CD spectral patterns and changes in patterns in KCl and urea, even though the spectra of Dz31 were rather complicated. Since the patterns of CD spectra were due, apparently, to parallel four-stranded quadruplexes that were associated with the formation of G-quadruplexes, it seems likely that the upper bands were due to the complexes that consisted of parallel four-stranded quadruplexes.

In contrast to the above-described results, D10-(G8A) did not form an upper band on the gel (Figure 2A) and did not yield a CD spectrum typical of a parallel four-stranded quadruplex (Figure 3D). This result was to be expected since D10-(G8A) did not include five adjacent guanosine nucleotides: the middle guanosine was replaced by adenosine and the formation of a G-quadruplex was inhibited. Comparing the CD spectra and results of electrophoresis for Dz31 and D10 with those for Dz31-(G8A) and D10-(G8A), we can clearly see that four or more adjacent guanosine nucleotides are responsible for the formation of a G-quadruplex by the DNA enzyme.

## Interference in reactions by the G-quadruplex

The sequences of the DNA enzymes and the substrates that bind through Watson–Crick base pairing are shown in Figure 1. We found earlier that Dz31, which is 31 nt long, was the most effective DNA enzyme; it cleaved the substrate between the indicated guanosine and cytidine residues of *b2a2* mRNA (14,15). To investigate the influence of the G-quadruplex on catalysis by the DNA enzyme, we prepared two analogs, Dz31-(G8A) and Dz31-(G8deaza). Dz31-(G8A) included adenosine instead of guanosine at position 8 in Dz31. The replacement of G by A in the middle of the five adjacent guanosine residues hinders the formation of a parallel four-stranded quadruplex. Dz31-(G8deaza) had an $N^7$-deaza-guanosine moiety at position 8 and it too failed to yield an upper band on gels (Figure 2B). D10-(G8A) also did not produce CD patterns characteristic of the formation of a G-quadruplex (Figure 3D). We adjusted the substrate of Dz31-(G8A), by changing C to U, to allow the formation

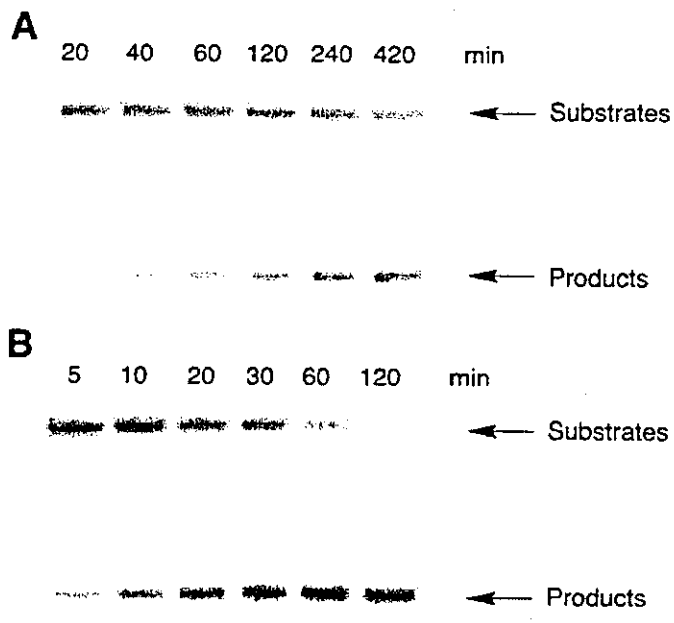


**Figure 4.** Autoradiograms showing the products of reactions in the presence of 25 mM $Mg^{2+}$ at 37°C: (**A**) 50 mM Tris (pH 8.0) with catalysis by Dz31; (**B**) 50 mM Bis-Tris (pH 6.0) with catalysis by Dz31-(G8A).

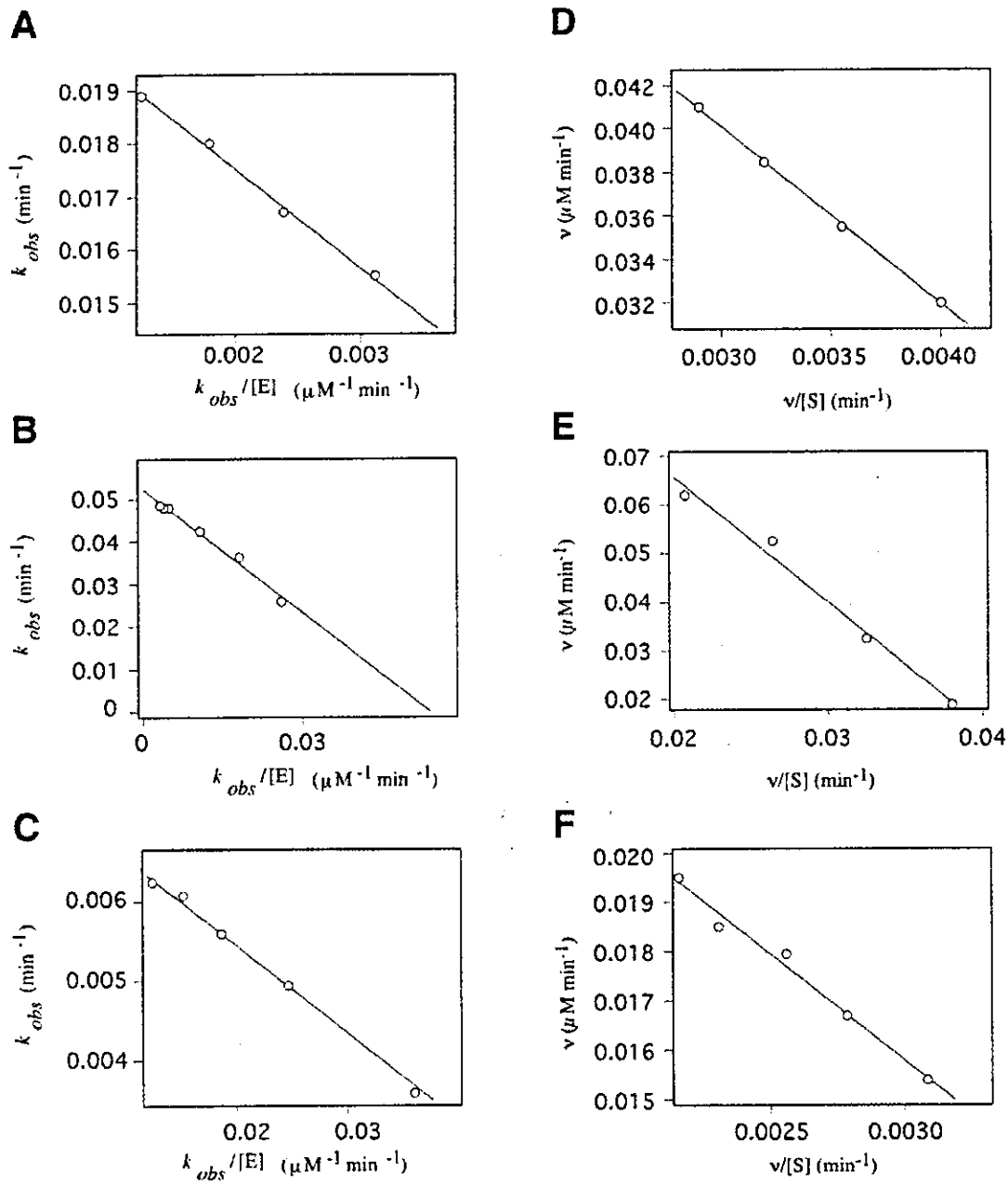


**Figure 5.** Determination of kinetic parameters from the equation $k_{obs} = k_{cleav} - (k_{obs} \times K_d)/[E]$ (A–C) and Eadie–Hofstee plots (D–F). Reactions were performed in the presence of 25 mM $Mg^{2+}$ at 37°C, under single-turnover conditions (A–C) and in the presence of 25 mM $Mg^{2+}$ in 50 mM Tris (pH 8.0), at 37°C under multiple-turnover conditions (D–F). (A) Kinetic data for Dz31 were obtained from reactions in 50 mM of Tris (pH 8.0) and yielded a $K_m$ of 1.89 μM and a $k_{cat}$ of 0.02 $min^{-1}$. (B) Values of $K_m$ of 0.96 μM and of $k_{cat}$ of 0.05 $min^{-1}$ were obtained for Dz31-(G8A) from reactions in 50 mM of Bis-Tris (pH 6.0). (C) Kinetic data for Dz31-(G8deaza) were obtained from reactions in 50 mM Tris (pH 8.0) and yielded a $K_m$ of 0.11 μM and a $k_{cat}$ of 0.016 $min^{-1}$. (D) Data for Dz31 yielded a $K_m$ of 8.2 μM and a $k_{cat}$ of 0.05 $min^{-1}$. (E) Data for Dz31-(G8A) yielded a $K_m$ of 2.93 μM and a $k_{cat}$ of 2.35 $min^{-1}$. (F) Data for Dz31-(G8deaza) yielded a $K_m$ of 4.3 μM and a $k_{cat}$ of 0.10 $min^{-1}$.

of a base pair between Dz31-(G8A) and its substrate [b2a2-(C10U)] (Figure 1).

We calculated the kinetic parameters of the DNA enzymes by performing RNA-cleavage reactions under single- and multiple-turnover conditions. The cleavage products were analyzed by electrophoresis on a 20% polyacrylamide/7 M urea denaturing gel, as shown in Figure 4. The reactions with Dz31 and Dz31-(G8deaza) under single-turnover conditions were performed in 50 mM Tris–HCl (pH 8.0) plus 25 mM $Mg^{2+}$ at 37°C. We used a lower pH, namely pH 6.0, for Dz31-(G8A) in order to slow down the rates of reactions so that we could make accurate measurements of kinetic parameters under single-turnover conditions in 50 mM Bis-Tris–HCl (pH 6.0). To obtain the kinetic parameters $K_m$ and $k_{cat}$ under single-turnover conditions, we used the equation $k_{obs} = k_{cleav} - (k_{obs} \times K_d)/[E]$ (Figure 5A–C) and the results are summarized in Table 1.

The mixtures for multiple-turnover reactions contained 0.5–10 μM DNA enzyme [Dz31 or Dz31-(G8deaza)] plus 1–50 μM b2a2 mRNA and 0.05–1 μM Dz31-(G8A) plus

**Table 1.** Kinetic parameters of cleavage of an RNA (17mer) substrate

| Enzyme | Substrate | $k_{cat}$ ($min^{-1}$) | $K_m$ (μM) |
|---|---|---|---|
| Dz31 (31mer) | b2a2 (17mer) | 0.020 ± 0.003 | 1.89 ± 0.35 |
| Dz31-(G8A) (31mer)[a] | b2a2-(C10U) (17mer) | 0.050 ± 0.003 | 0.96 ± 0.12 |
| Dz31-(G8deaza) (31mer) | b2a2 (17mer) | 0.016 ± 0.001 | 0.11 ± 0.02 |

Determined in 50 mM of Tris–HCl (pH 8.0) and 25 mM of $MgCl_2$ under enzyme-saturating (single-turnover) conditions at 37°C.
[a]pH was 6.0.

**Table 2.** Kinetic parameters of cleavage of an RNA (17mer) substrate

| Enzyme | Substrate | $k_{cat}$ ($min^{-1}$) | $K_m$ (μM) |
|---|---|---|---|
| Dz31 (31mer) | b2a2 (17mer) | 0.050 ± 0.013 | 8.20 ± 0.30 |
| Dz31-(G8A) (31mer) | b2a2-(C10U) (17mer) | 2.34 ± 0.02 | 2.93 ± 0.35 |
| Dz31-(G8deaza) (31mer) | b2a2 (17mer) | 0.10 ± 0.01 | 4.30 ± 0.51 |

Determined in 50 mM of Tris–HCl (pH 8.0) and 25 mM of $MgCl_2$ under multiple-turnover conditions at 37°C.

0.5–15 μM b2a2-(C10U) mRNA. All these reactions were performed in 50 mM Tris–HCl (pH 8.0) plus 25 mM $Mg^{2+}$ ions at 37°C. Cleavage rates were obtained from the initial slopes of the curves of the time courses of reactions, and $K_m$ and $k_{cat}$ were calculated from Eadie–Hofstee plots (Figure 5D–F). The results are summarized in Table 2.

The $K_m$ values of Dz31-(G8deaza) and Dz31-(G8A) were smaller than that of Dz31, as shown in Tables 1 and 2. Since Dz31-(G8deaza) and Dz31-(G8A) do not form quadruplexes, they can bind easily to their substrates. In contrast, Dz31 can form a quadruplex and, thus, the association of the DNA enzyme with its substrate is impaired. Since the preformed G-quadruplex seemed to be extremely stable (inert), it is difficult to unfold Dz31-quadruplex to accommodate its substrate RNA (33). As a result, the observed $K_m$ of Dz31 was larger than those of Dz31-(G8deaza) and Dz31-(G8A). The $k_{cat}$ value of Dz31-(G8deaza) was similar to that of Dz31, as shown in Tables 1 and 2. This result is reasonable since $k_{cat}$ reflects the cleavage rate under saturating conditions, implying that the formation of a G-quadruplex does not affect the chemical step during cleavage.

The $k_{cat}$ value of Dz31-(G8A) was much higher than that of Dz31 and Dz31-(G8deaza), as shown in Figure 4 and summarized in Tables 1 and 2. The cleavage reaction catalyzed by Dz31-(G8A) was too fast for measurements of kinetic parameters at pH 7 and 8, and the reaction seemed to be pH dependent, as is the case for reactions catalyzed by hammerhead ribozymes (3,34). The difference between the reactions catalyzed by Dz31-(G8deaza) and Dz31-(G8A) involves the difference in sequence at position 8 in the DNA enzyme and the complementary sequence in the substrate. In the former case, there is an $N^7$-deazaG–C base pair and in the latter case there is an A–U base pair. In neither case does a quadruplex form. The different base pairs produce extremely different $k_{cat}$ values that reflect the chemical step during cleavage. It is possible that the combination of the A–U base pair moves the conformation in the vicinity of the catalytic site closer to the transition state with lower energy and, thus, the A–U base pair is more effective than the G–C base pair at this position (35).

It seems probable that the difference in kinetic parameters between Dz31 and Dz31-(G8A), as shown in Tables 1 and 2, was due to at least two factors: (i) the formation of a G-quadruplex, which affects $K_m$ and (ii) the conformation in the transition state, which affects $k_{cat}$.

## CONCLUSION

We have analyzed in detail the formation of quadruplexes by DNA oligomers. Adjacent G residues, even if they are within the catalytic site of the DNA enzyme, form a G-quadruplex, as indicated by gel mobility, CD measurements and kinetic parameters. Addition of negative charges (phosphorylation) to the ends of G-quadruplex-forming oligomers inhibited dimerization of G-quadruplexes. To our knowledge, this is the first example of inhibition of the dimerization of G-quadruplexes by direct phosphorylation of a continuous terminal stretch of G residues. Furthermore, we compared the catalytic activities of Dz31 and its mutant derivatives, such as Dz31-(G8A) and Dz31-(G8deaza), in which hydrogen bonding within the stretch of G residues was disrupted. The values of $k_{cat}$ for Dz31 and Dz31-(G8deaza) were almost the same under single-turnover conditions, but Dz31-(G8deaza) was a slightly more efficient catalyst under multiple-turnover conditions, reflecting the presence of a higher concentration of a more reactive species in the latter case. Dz31-(G8A), which did not form a G-quadruplex and possessed the favorable A–U base pair, was 50 times more reactive than Dz31 and Dz31-(G8deaza). Reflecting the formation of a G-quadruplex, Dz31 had a significantly higher $K_m$ than Dz31-(G8A) and Dz31-(G8deaza). As expected, G-quadruplexes within DNA enzymes inhibited catalysis and, thus, selection of corresponding target sequences should be avoided in an effort to maintain high rates of cleavage by DNA enzymes.

## ACKNOWLEDGEMENTS

The authors thank Ms Clair Price for critical reading of the manuscript. M.K.U. was supported by the Japan Society for the Promotion of Science (JSPS).

## REFERENCES

1. Bock,L.C., Griffin,L.C., Latham,J.A., Vermaas,E.H. and Toole,J.J. (1992) Selection of single-stranded DNA molecules that bind and inhibit human thrombin. *Nature*, **355**, 564–566.
2. Ellington,A.D. and Szostak,J.W. (1992) Selection *in vitro* of single-stranded DNA molecules that fold into specific ligand-binding structures. *Nature*, **355**, 850–852.
3. He,Q.-C., Zhou,J.-M., Zhou,D.-M., Nakamatsu,Y., Baba,T. and Taira,K. (2002) Comparison of metal-ion-dependent cleavages of RNA by a DNA enzyme and a hammerhead ribozyme. *Biomacromolecules*, **3**, 69–83.
4. Cuenoud,B. and Szostak,J.W. (1995) A DNA metalloenzyme with DNA ligase activity. *Nature*, **375**, 611–614.
5. Carmi,N., Shultz,L.A. and Breaker,R.R. (1996) *In vitro* selection of self-cleaving DNAs. *Chem. Biol.*, **3**, 1039–1046.

6. Li,Y. and Sen,D. (1997) Toward an efficient DNA enzyme. *Biochemistry*, **36**, 5589–5599.
7. Li,Y. and Breaker,R.R. (1999) Deoxyribozymes: new players in the ancient game of biocatalysis. *Curr. Opin. Struct. Biol.*, **9**, 315–323.
8. Li,Y., Liu,Y. and Breaker,R.R. (2000) Capping DNA with DNA. *Biochemistry*, **39**, 3106–3114.
9. Feldman,A.R. and Sen,D. (2001) A new and efficient DNA enzyme for the sequence-specific cleavage of RNA. *J. Mol. Biol.*, **313**, 283–294.
10. Wang,D.Y., Lai,B.H.Y., Feldman,A.R. and Sen,D. (2002) A general approach for the use of oligonucleotide effectors to regulate the catalysis of RNA-cleaving ribozymes and DNA enzymes. *Nucleic Acids Res.*, **30**, 1735–1742.
11. Breaker,R.R. and Joyce,G.F. (1994) A DNA enzyme that cleaves RNA. *Chem. Biol.*, **1**, 223–229.
12. Santoro,S.W. and Joyce,G.F. (1997) A general purpose RNA-cleaving DNA enzyme. *Proc. Natl Acad. Sci. USA*, **94**, 4262–4266.
13. Cox,J.C., Cohen,D.S. and Ellington,A.D. (1999) The complexities of DNA computation. *Trends Biotechnol.*, **17**, 151–154.
14. Kuwabara,T., Warashina,M., Tanabe,T., Tani,K., Asano,S. and Taira,K. (1997) Comparison of the specificities and catalytic activities of hammerhead ribozymes and DNA enzymes with respect to the cleavage of *BCR-ABL* chimeric L6 (b2a2) mRNA. *Nucleic Acids Res.*, **25**, 3074–3081.
15. Warashina,M., Kuwabara,T., Nakamatsu,Y. and Taira,K. (1999) Extremely high and specific activity of DNA enzymes in cells with Philadelphia chromosome. *Chem. Biol.*, **6**, 237–250.
16. Santoro,S.W. and Joyce,G.F. (1998) Mechanism and utility of an RNA-cleaving DNA enzyme. *Biochemistry*, **37**, 13330–13342.
17. Nowell,P.C. and Hungerford,D.A. (1960) A minute chromosome in human chronic granulocytic leukemia. *Science*, **132**, 1497–1499.
18. Blackburn,E.H. (1994) Telomeres: no end in sight. *Cell*, **77**, 621–623.
19. Sen,D. and Gilbert,W. (1988) Formation of parallel four-stranded complexes by guanine-rich motifs in DNA and its implications for meiosis. *Nature*, **334**, 364–366.
20. Evans,T., Schon,E., Gora-Maslak,G., Patterson,J. and Efstratiadis,A. (1984) S1-hypersensitive sites in eukaryotic promoter regions. *Nucleic Acids Res.*, **12**, 8043–8058.
21. Kilpatrick,M.W., Torri,A., Kang,D.S., Engler,J.A. and Wells,R.D. (1986) Unusual DNA structures in the adenovirus genome. *J. Biol. Chem.*, **261**, 11350–11354.
22. Fry,M. and Loeb,L.A. (1994) The fragile X syndrome $d(CGG)_n$ nucleotide repeats form a stable tetrahelical structure. *Proc. Natl Acad. Sci. USA*, **91**, 4950–4954.
23. Williamson,J.R. (1993) Guanine quartets. *Curr. Opin. Struct. Biol.*, **3**, 357–362.
24. Williamson,J.R. (1994) G-quartet structures in telomeric DNA. *Annu. Rev. Biophys. Biomol. Struct.*, **23**, 703–730.
25. Keniry,M.A. (2001) Quadruplex structures in nucleic acids. *Biopolymers*, **56**, 123–146.
26. Henderson,E., Hardin,C.C., Walk,S.K., Tinoco,J.I. and Blackburn,E.H. (1987) Telomeric DNA oligonucleotides form novel intramolecular structures containing guanine–guanine base pairs. *Cell*, **51**, 899–908.
27. Gueschlbauer,W., Chantot,J.-F. and Thiele,D. (1990) Four-stranded nucleic acid structures 25 years later: from guanosine gels to telomer DNA. *J. Biomol. Struct. Dyn.*, **8**, 491–511.
28. Balagurumoorthy,P. and Brahmachari,S.K. (1994) Structure and stability of human telomeric sequence. *J. Biol. Chem.*, **269**, 21858–21869.
29. Penazova,H. and Vorlickova,M. (1997) Guanine tetraplex formation by short DNA fragments containing runs of guanine and cytosine. *Biophys. J.*, **73**, 2054–2063.
30. Protozanova,E. and Macgregor,R.,Jr (1996) Frayed wires: a thermally stable form of DNA with two distinct structural domains. *Biochemistry*, **35**, 16638–16645.
31. Sen,D. and Gilbert,W. (1992) Novel DNA superstructures formed by telomere-like oligomers. *Biochemistry*, **31**, 65–70.
32. Wang,Y. and Patel,D.J. (1992) Guanine residues in $d(T_2AG_3)$ and $d(T_2G_4)$ form parallel-stranded potassium cation stabilized G-quadruplexes with anti glycosidic torsion angles in solution. *Biochemistry*, **31**, 8112–8119.
33. Li,W., Miyoshi,D., Nakano,S. and Sugimoto,N. (2003) Structural competition involving G-quadruplex DNA and its complement. *Biochemistry*, **42**, 11736–11744.
34. Takagi,Y., Warashina,M., Stec,W.J., Yoshinari,K. and Taira,K. (2001) Recent advances in the elucidation of the mechanisms of action of ribozymes. *Nucleic Acids Res.*, **29**, 1815–1834.
35. Cairns,M.J., King,A. and Sun,L.-Q. (2003) Optimization of the 10–23 DNAzyme-substrate pairing interactions enhanced RNA cleavage activity at purine–cytosine target sites. *Nucleic Acids Res.*, **31**, 2883–2889.